Computational and Structural Biotechnology Journal 21 (2023) 1606–1620

Contents lists available at ScienceDirect

Computational and Structural Biotechnology Journal

journal homepage: www.elsevier.com/locate/csbj

Short-chain fatty acids reprogram metabolic profiles with the induction of reactive oxygen species production in human colorectal adenocarcinoma cells

Chongyang Huang [a,1], Wenjun Deng [b,1], Huan-zhou Xu [e], Chen Zhou [b], Fan Zhang [f], Junfei Chen [a], Qinjia Bao [a,c], Xin Zhou [a,c,d], Maili Liu [a,c,d], Jing Li [b,c,*], Chaoyang Liu [a,c,d,**]

[a] State Key Laboratory of Magnetic Resonance and Atomic and Molecular Physics, Innovation Academy for Precision Measurement Science and Technology, Chinese Academy of Sciences, Wuhan, China
[b] Wuhan Botanical Garden, Chinese Academy of Sciences, Wuhan, Hubei, China
[c] University of Chinese Academy of Sciences, Beijing, China
[d] Optics Valley Laboratory, Hubei 430074, China
[e] Department of Pediatrics, Division of Infectious Diseases, College of Medicine, University of Florida, Gainesville, FL, USA
[f] Wuhan Institute of Virology, Chinese Academy of Sciences, Wuhan, China

ARTICLE INFO

Article history:
Received 5 January 2023
Received in revised form 10 February 2023
Accepted 11 February 2023
Available online 13 February 2023

Keywords:
Short-chain fatty acids
Mitochondrial function
NMR-based Metabolomics
Transcriptomics
Reactive oxygen species

ABSTRACT

Short-chain fatty acids (SCFAs) exhibit anticancer activity in cellular and animal models of colon cancer. Acetate, propionate, and butyrate are the three major SCFAs produced from dietary fiber by gut microbiota fermentation and have beneficial effects on human health. Most previous studies on the antitumor mechanisms of SCFAs have focused on specific metabolites or genes involved in antitumor pathways, such as reactive oxygen species (ROS) biosynthesis. In this study, we performed a systematic and unbiased analysis of the effects of acetate, propionate, and butyrate on ROS levels and metabolic and transcriptomic signatures at physiological concentrations in human colorectal adenocarcinoma cells. We observed significantly elevated levels of ROS in the treated cells. Furthermore, significantly regulated signatures were involved in overlapping pathways at metabolic and transcriptomic levels, including ROS response and metabolism, fatty acid transport and metabolism, glucose response and metabolism, mitochondrial transport and respiratory chain complex, one-carbon metabolism, amino acid transport and metabolism, and glutaminolysis, which are directly or indirectly linked to ROS production. Additionally, metabolic and transcriptomic regulation occurred in a SCFAs types-dependent manner, with an increasing degree from acetate to propionate and then to butyrate. This study provides a comprehensive analysis of how SCFAs

Abbreviations: NMR, Nuclear Magnetic Resonance; SCFAs, Short Chain Fatty Acids; ROS, Reactive Oxygen Species; HT29, Human Colorectal Adenocarcinoma Cell Line with Epithelial Morphology; HCT116, Human Colorectal Carcinoma Cell Line; Caco-2, Human Colon Adenocarcinoma; WST-1, Water-Soluble Tetrazolium salts; DMEM, Dulbecco's Modified Eagle Medium; DCFH-DA, Dichloro-Dihydro-Fluorescein Diacetate; EP, Eppendorf; NOESY, Nuclear Overhauser Effect Spectroscopy; J-Res, J-resolved Spectroscopy; ^{1}H–^{1}H COSY, ^{1}H–^{1}H Correlation Spectroscopy; ^{1}H–^{1}H TOCSY, ^{1}H–^{1}H Total Correlation Spectroscopy; ^{1}H–^{13}C HSQC, ^{1}H–^{13}C Heteronuclear Single Quantum Coherence Spectroscopy; ^{1}H–^{13}C HMBC, ^{1}H–^{13}C Heteronuclear Multiple Bond Correlation Spectroscopy; PCA, Principal Component Analysis; O-PLS-DA, Orthogonal Projection to the Latent Structures Discriminant Analysis; RNA, Ribonucleic Acid; DNA, Deoxyribonucleic Acid; qRT-PCR, Real-Time Quantitative Reverse Transcription Polymerase Chain Reaction; GSEA, Gene Set Enrichment Analysis; RPKM, Reads per Kilobase of Transcript per Million Reads Mapped; FDR, False Discovery Rate; DEGs, Differentially Expressed Genes; CoA, Coenzyme A; SLC, Solute-Carrier Genes; HEK, Human Embryonic Kidney cells; CRC, Colorectal Cancer; TCA, Tricarboxylic Acid; MCF-7, Human Breast Cancer Cell Line with Estrogen; PKC, Protein Kinase C; GLS, Glutaminase; MCT, Monocarboxylate Transporters; MetS, Metabolic Syndrome; T2DM, Type 2 Diabetes; PDK, Pyruvate Dehydrogenase Kinase; PDC, Pyruvate Decarboxylase; LDH, Lactate Dehydrogenase; PPP, Pentose Phosphate Pathway; dDNP, dissolution Dynamic Nuclear Polarization; PA, Pantothenate; Ile, Isoleucine; Leu, Leucine; Val, Valine; α-KMV, α-keto-β-methyl-valerate; α-KIV, α-Keto-isovalerate; Lac, Lactate; Thr, Threonine; Ala, Alanine; NAG, *N*-Acetyl-L-Glutamine; Glu, Glutamate; Gln, Glutamine; Pyr, Pyruvate; Suc, Succinate; Met, Methionine; DMG, Dimethylglycine; GSH, Glutathione; Cre, Creatine; Cho, Choline; PC, Phosphocholine; Tau, Taurine; Fru, Fructose; Glc, Glucose; Gal-1-P, Galactose-1-phosphate; Fum, Fumaric acid; Tyr, Tyrosine; Phe, Phenylalanine; UMP, Uridine 5′-monophosphate; His, Histidine; NAD^{+}, Nicotinamide adenine dinucleotide; FA, Formate; AMP, Adenosine monophosphate; ATP, Adenosine triphosphate; UDP, Uridine 5′-diphosphate; UDP-GLC, UDP Glucose; UDPG, UDP Glucuronate; UDPGs, UDP Glucose and UDP Glucuronate; Ace, Acetate; Lys, Lysine; Gly, Glycine; ADP, Adenosine diphosphate; Ach, Acetylcholine

* Corresponding author at: Wuhan Botanical Garden, Chinese Academy of Sciences, Wuhan, Hubei, China.
** Corresponding author at: State Key Laboratory of Magnetic Resonance and Atomic and Molecular Physics, Innovation Academy for Precision Measurement Science and Technology, Chinese Academy of Sciences, Wuhan, China.
E-mail addresses: lijing@wbgcas.cn (J. Li), chyliu@apm.ac.cn (C. Liu).
[1] These authors contributed equally to this work.

https://doi.org/10.1016/j.csbj.2023.02.022

induce ROS production and modulate metabolic and transcriptomic levels in colon cancer cells, which is vital for understanding the mechanisms of the effects of SCFAs on antitumor activity in colon cancer.

1. Introduction

A gut ecosystem consisting of a dynamic and complex microbiota [1] is regarded as a separate organ system for its interaction with the host and integration into the host biology [2]. Colon cancer is closely associated with diet habits [3]. Short-chain fatty acids (SCFAs), including acetate, propionate, and butyrate [4], are produced by the gut microbiota through the fermentation of dietary fibers [5] and have been reported to play essential roles in the communication between the gut and microbes, in the interconnection of the gut-brain axis of the microbiota [6], and most critically, in the inhibition of colon tumor progression [7].

A previous study has shown that SCFAs induce apoptotic cell death and activate autophagic responses in colon cancer cells [3]. Butyrate, known to be the most effective SCFA in maintaining intestinal barrier function [8,9], exerts extraordinary anticancer activities [10] and is the most studied SCFA [11,12] in terms of inhibiting the progression and proliferation of cancer cells by regulating metabolic, endocrine, and immune functions [13]. However, acetate and propionate have received considerable attention because of their potential benefits in nutrient absorption, inflammation inhibition, and tumor growth inhibition [3]. Acetate, accounting for approximately 60–75% of the total fecal SCFAs [14], has been demonstrated to have anti-tumorigenic effects after being delivered in liposomes [15] and induce colon cancer cell death when combined with propionate [16]. Acetate inhibits the proliferation of human cancer cell lines, HT29 and HCT116, by reducing glycolysis and increasing reactive oxygen species (ROS) levels [17]. Moreover, propionate suppresses colon cancer growth by promoting the proteasomal degradation of euchromatic histone-lysine *N*-methyltransferase 2 [18]. In addition to research on a single SCFA, the combination of butyrate and propionate induced a greater extent of apoptosis and G2-M arrest than propionate alone in Caco-2 cells. However, butyrate induced a higher oxidative pentose pathway activity than SCFAs combination treatment for 24 and 48 h [19].

The mechanisms involved in colon cancer inhibition include inhibition of glycolysis, activation of ROS production, transformation of the redox state, histone acetylation, induction of apoptosis by differentiation, and regulation of the expression of various oncogenes. These three main SCFAs showed different effects on the inhibition of colon cancer. Butyrate shows greater inhibitory efficacy than propionate and acetate against HCT116 cell line proliferation through cell cycle arrest and apoptosis [20]. Furthermore, acetate and propionate can modulate the barrier function of Caco-2 monolayers at higher concentrations than butyrate [21]. It has been hypothesized that chain length determines the bioactivity of SCFAs in inflammation, carcinogenesis, and barrier function [22–25]. DeSoignie et al. found that lipid solubility decreases as the chain length decreases, which influences the ability of SCFAs to cross cell membranes [24].

Although several studies have attempted to understand the precise mechanisms by which SCFAs affect colon cancer, the comprehensive pathways through which SCFAs induce apoptosis and growth arrest in colon cancer cells remain unclear. However, cancer has been suggested to be both a genetic and metabolic disease [26]. According to this theory, metabolic disturbances in cancer cells would induce ROS accumulation, leading to biomolecular damage and cell death, and vice versa. Although several studies have focused on one or more metabolites or genes involved in specific pathways related to human cancer progression, additional systematic investigations are needed to elucidate the overall mechanism by which SCFAs inhibit cancer cell proliferation. In this study, we investigated the molecular basis by which acetate, propionate, and butyrate interact with human colorectal adenocarcinoma cells at physiological concentrations, by combining metabolomic and transcriptomic analyses. Additionally, we analyzed the effects of SCFAs treatments on ROS production. We aimed to provide a comprehensive analysis of the processes by which SCFAs affect colon cancer progression.

2. Experiment and design

2.1. Caco-2 cells culture and cell viability assay

Caco-2 cells (ATCC #HTB-37) were maintained and cultured in Minimum Essential Medium (MEM) containing 20% fetal bovine serum, 1% penicillin-streptomycin, 1x non-essential amino acid solution, and 10 mM sodium pyruvate at 37 °C and 5% CO_2.

Cell viability was determined using the WST-1 assay, according to the manufacturer's protocol (Beyotime, Shanghai, China). Briefly, human colon epithelial cells (Caco-2) were seeded in a 96-well plate (1×10^4 cells/well) and cultured in a humidified CO_2 incubator with 5% CO_2 at 37 °C. After 24 h of incubation, the cells were treated with various concentrations of acetate, propionate, and butyrate (0, 2.5, 5, 10, 20, 40, 80, 160, and 320 mM, Sigma-Aldrich) for 24 h. WST-1 reagent was added to each well, and the plate was incubated for 2 h at 37 °C. The absorbance was measured at 450 nm using a microplate reader (TECAN M200 PRO, Switzerland).

2.2. Measurement of ROS generation

After 24 h-incubation, the cells were treated with low concentrations of SCFAs (acetate, 20 mM; propionate, 5 mM; and butyrate, 3 mM) and high concentrations of SCFAs (acetate, 80 mM; propionate, 20 mM; and butyrate, 12 mM), and MEM was used as the control treatment. After treatments, the cells were incubated with 10 μM 2′, 7′-dichlorodihydrofluorescein diacetate (DCFH-DA) solution for 20 min at 37 °C. Subsequently, the cells were washed three times with serum-free MEM to completely remove DCFH-DA. Two methods were used for ROS detection using a ROS assay kit (Beyotime, Shanghai, China). First, Caco-2 cells were treated with different concentrations of SCFAs to detect the fluorescence intensity of ROS at 488 nm excitation and 525 nm emission wavelengths using a microplate reader (TECAN M200 PRO, Switzerland). Relative fluorescence was calculated using the following formula: relative fluorescence (%) = $\frac{Treatmentgroup}{controlgroup} \times 100\%$. Fluorescence images of ROS from the high-concentration SCFA-treated and control cells were obtained using a laser confocal microscope (Leica TCS SP8, Germany) and measured at 488 nm excitation and 525 nm emission wavelengths.

2.3. Sample collection and preparation for metabolic analysis

Caco-2 cells were incubated with sodium acetate (20 mM), sodium propionate (5 mM), and sodium butyrate (3 mM). After 24 h of

incubation, the medium was removed from the cell culture flask, and the cells were washed twice with 2 mL water and then quenched with liquid N_2. The cells were stored at − 80 °C until extraction for nuclear magnetic resonance (NMR) detection. Methanol:water extraction methods were conducted according to a previously described protocol [27]: 1 mL extraction solution of 80% methanol was added to the cell culture flask, and cells were scraped into a 2-mL EP tube followed by two sonication and vortex cycles. The mixtures were then centrifuged for 45 min at 12000 × *g* at 4 °C, and the supernatant was collected in a 2-mL EP tube. Methanol was removed using a spin vac, and water was removed by freeze-drying. The dry extracted powder was stored at − 80 °C until NMR detection.

2.4. NMR experiment and data analysis

The extracts were redissolved in 520 μL phosphate buffer (0.1 M K_2HPO_4/NaH_2PO_4 in D_2O, pD 7.4). Particulates were removed by centrifugation (5 min, 12000 × *g*, 4 °C), and 500 μL of the supernatant was pipetted into a 5.0-mm NMR tube. An 800-MHz Bruker Avance III NMR system (Bruker BioSpin, Germany) equipped with a 5-mm TCI cryoprobe was used to acquire one-dimensional ^{1}H NMR spectra at 25 °C with a water-suppressed 1D-NOESY sequence using a 100-ms mixing time [28]. Sixty-four scans were collected for each spectrum using a 5 s relaxation delay, 120190 points, and a 12-kHz sweep width. Five two-dimensional spectra, namely ^{1}H–^{1}H J-resolved (J-Res), ^{1}H–^{1}H correlation spectroscopy (COSY), ^{1}H–^{1}H total correlation spectroscopy (TOCSY), ^{1}H–^{13}C heteronuclear single quantum coherence spectroscopy (HSQC), and ^{1}H–^{13}C heteronuclear multiple bond correlation spectroscopy (HMBC) were acquired for a subset of control samples for assignment purposes.

The free induction decays were processed on Topspin 3.6.1 (Bruker BioSpin, Germany), multiplied by a 1 Hz exponential window function, Fourier transformed, and manually corrected for phase and minor baseline distortions. The spectra corresponded to the right doublet peak of lactate, with a chemical shift at δ 1.32, 2793 spectral peaks between 0.6 and 9.5 ppm were obtained with a uniform bucketing (bucket width = 0.002) method using the online software, NMRPROCFLOW (https://nmrprocflow.org). We removed the water regions (δ 4.65 −5.0) to avoid the effects of imperfect water suppression. Additionally, signals from acetate (δ 1.822 −2.0), propionate (δ 1.025–1.08 and δ 2.094–2.21), butyrate (δ 0.84–0.915, δ 1.516–1.6, and δ 2.094–2.20) and methanol (extraction solvent residual, δ 3.347–3.369) were excluded from the cell extraction spectra. We normalized the binning data using a probabilistic quotient normalization method and then scaled them to unit variance before performing multivariate analysis on the dataset on MetaboAnalyst [29] (https://www.metaboanalyst.ca/). Subsequently, we conducted a principal component analysis (PCA) on the dataset to generate an overview of the metabolic effects of acetate, propionate, and butyrate exposure. We incorporated back-transformed loadings from orthogonal projection to latent structures discriminant analysis (O-PLS-DA) with color-coded coefficients to generate coefficient plots in MATLAB (MATLAB & SIMULINK R2014a) [30]. The loading coefficients represent the weights of metabolites contributing to the separation between classes, where the red color indicates significance in the differentiation between the two groups and the blue color indicates no significance. We chose correlation coefficients higher than 0.878 as significant in the discrimination based on the 95% confidence limit and the number of samples in each group.

2.5. RNA sequencing (RNA-Seq)

Caco-2 cells were treated with 20 mM sodium acetate, 5 mM sodium propionate, or 3 mM sodium butyrate. Subsequently, the RNeasy Plus Mini Kit (Qiagen) was used to extract the total RNA from the cells. An RNA-seq library was constructed using total RNA with 28 S/18 S > 1 and RNA integrity numbers of 7.1–9.3. A SMART-Seq HT kit (Takara Bio) was used to generate cDNA. Finally, the Nextera DNA Flex Library Prep kit and Nextera DNA Unique Dual Indexes Set A (Illumina) were used to construct RNA-seq libraries. Quality control of the libraries (checking the size distribution with an average fragment size of 600 bp when analyzed with a size range of 150–1500 bp) and quantitative PCR (qPCR) assays (starting concentration: 2 nM and final loading concentration: 300 pM) were performed on the TapeStation. Finally, the libraries were sequenced using a NovaSeq6000 (Illumina).

RNA sequencing was performed using the CLC Genomics Workbench (Qiagen 21.0.4). Data were normalized to reads per kilobase of transcript per million mapped reads (RPKM). A false discovery rate (FDR)-corrected *p*-value was used as the criterion for significance. The outliers of the transcriptomes of all samples were evaluated using PCA on SIMCA 17.01. Gene set enrichment analysis (GSEA) was carried out with iDEP V0.94 using the pre-ranked fgsea method [31], and heat maps of differentially expressed genes (DEGs) in enriched pathways were built using supervised hierarchical clustering in Heatmapper [32].

2.6. Quantitative real-time reverse transcription polymerase chain reaction (qRT-PCR) assay

Caco-2 cells were treated with 20/80 mM acetate, 5/20 mM propionate, or 3/12 mM butyrate in a humidified CO_2 incubator with 5% CO_2 at 37 °C for 24 h. Total cell RNA was extracted using a MolPure® Cell RNA kit (Yeasen, Shanghai, China), following the manufacturer's protocol, and reverse-transcribed into cDNA using a reverse transcription kit (Vazyme, Nanjing). The qPCR primer sequences (Supplementary Table 2) were synthesized by Tsingke Biotech (Wuhan, China). qRT-PCR was performed using a QuantStudio 6 detection system (Applied Biosystems, USA) with a 10 μL reaction system containing Hieff® qPCR SYBR Green Master Mix (Yeasen, Shanghai, China). mRNA expression levels relative to *GAPDH* were calculated using the $2^{-\Delta\Delta CT}$ method.

3. Results

3.1. Effect of SCFAs on Caco-2 cell growth

Colon epithelial cells were selected to investigate the metabolic and transcriptomic effects of acetate, propionate, and butyrate, which account for more than 95% of SCFAs in the gut and colon at physiological concentrations. The physiological concentrations of SCFAs, including acetate, propionate, and butyrate, are approximately 50–150 mM in the colon [33]. The molar ratio of the SCFAs concentrations of acetate, propionate, and butyrate in the colon of postmortem human subjects is approximately 60:20:20 [34]. However, the concentrations of short fatty acids fluctuate under different physiological conditions in the gut. Cytotoxicity assays were performed to determine non-cytotoxic concentrations of SCFAs in Caco-2 cells. As shown in Fig. 1, cell viability gradually decreased with increasing concentrations of SCFAs compared with the corresponding control group.

Additionally, different SCFAs treatments resulted in different cytotoxicities. For example, 2.5–80 mM of acetate had no noticeable cytotoxic effect on Caco-2 cells, whereas acetate concentrations higher than 80 mM were cytotoxic. However, the non-cytotoxic concentrations of propionate and butyrate were up to 40 mM and 20 mM, respectively, suggesting that these two SCFAs were more toxic than acetate in Caco-2 cells (Fig. 1). Summarizing these results and previous reports on the physiological concentrations of SCFAs in the gut [33], we investigated the effect of 20 mM acetate, 5 mM

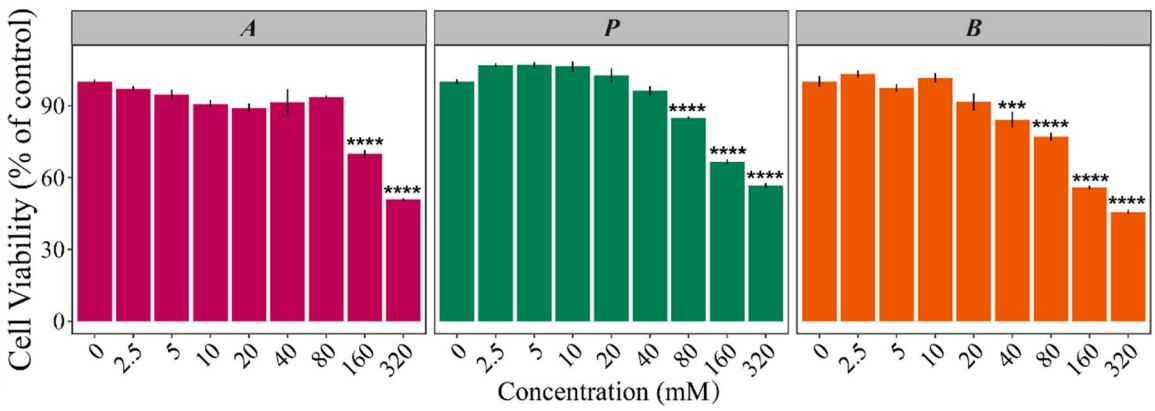

Fig. 1. Effects of SCFAs on cell viability in Caco-2 cells. Data are expressed as mean ± SD (n = 4). The statistical analysis was performed between the control and treatments using a one-way ANOVA with Dunnett's multiple comparisons test. * ** represents $p < 0.001$, and * *** * represents $p < 0.0001$. A: acetate; P: propionate; B: butyrate.

propionate, or 3 mM butyrate treatment on ROS production and metabolomic and transcriptomic profiles of Caco-2 cells.

3.2. SCFAs activated the intracellular production of ROS

Our previous RNA-seq data demonstrated that lactate, a microbial metabolite like the SCFAs, significantly upregulated ROS metabolism and disturbed mitochondrial function by downregulating the electron transport chain and oxidative phosphorylation in Caco-2 cells [35], which endogenously generated ROS in the mitochondria [4]. Consistently, ROS-mediated fluorescence was significantly promoted by increasing the concentrations of SCFAs (Fig. 2A), indicating that the enhancement of ROS production by SCFAs was dose-dependent in Caco-2 cells. Of the mentioned SCFAs, propionate was the most potent enhancer of ROS biosynthesis (Fig. 2A). Additionally, laser confocal microscopy showed an obvious induction of ROS production in cells treated with high concentrations of SCFAs (Fig. 2B).

3.3. Metabolite assignments for ^{1}H NMR spectroscopy

Fig. 3 shows the typical ^{1}H NMR spectra of the cell extracts obtained from the control group. Metabolite assignments were confirmed using two-dimensional NMR spectra and verified using data reported in the literature [36]. In total, 41 metabolites were identified. Signals arose at the high field between 0.00 ppm and 4.6 ppm mainly including amino acids (e.g., glutamine, valine, isoleucine, and leucine), sugars (e.g., glucose and fructose), and a range of organic acids (e.g., lactate and succinate). Additionally, nucleotides (e.g., adenosine monophosphate, adenosine triphosphate, uridine 5′-monophosphate, and uridine-5′-diphosphate) were found in the low field between 5.00 ppm and 9.4 ppm. More detailed assignments of metabolites are provided in Supplementary Table 1.

3.4. Significantly changed metabolites detected by high-resolution ^{1}H NMR

PCA score plots displayed distinguishing metabolic profiles of exposure to acetate, propionate, and butyrate compared to the control group. Overall, butyrate induced more distinct metabolic disturbances (Fig. 4C) than propionate (Fig. 4 B). Acetate had an almost negligible effect on Caco-2 cells (Fig. 4A). Twelve significantly changed metabolites, including six with increased leucine, glycine, phenylalanine, tyrosine, choline, fructose, acetylcholine, and six with decreased ATP/ADP, lactate, choline, UDP glucuronate, and UDP glucose (UDPGs), were observed in all three treatments (Fig. 4 D and E). Signatures changed in the propionate and butyrate treatment groups, including elevated levels of acetate, glucose, α-keto-β-methyl-valerate (α-KMV), isoleucine, succinate, nicotinamide adenine dinucleotide (NAD^+), and reduced levels of glutathione (GSH), phosphocholine (PC), and taurine.

Increased α-Keto-isovalerate (α-KIV) levels were observed only in the propionate group. Butyrate treatment also resulted in some metabolic alterations, including increased lysine, glutamine, histidine, dimethylglycine (DMG), alanine, *N*-Acetyl-L-Glutamine (NAG), pyruvate, and valine levels and decreased creatine and methionine levels. Furthermore, glutamate, which plays a critical role in the central metabolism of many organisms, showed significantly higher levels in the acetate group, but significantly lower levels in the butyrate group (Fig. 4 D).

Additionally, several intracellular metabolic signatures changed depending on the type of SCFAs used. Corresponding plots of normalized concentrations (Fig. 5) for the respective SCFAs types were plotted, and gradually increased the production levels of Ile, Leu, Val, Gln, Lys, Tyr, His, Phe, Glc, Fru, Pyr, DMG, and Tau were observed in the order of acetate, propionate, and then butyrate at their physiological concentrations. Meanwhile, ATP/ADP, UDPGs, GSH, Cre, PC, and Cho were dropped off by acetate, propionate, and then butyrate treatment.

3.5. SCFAs modulated transcriptome signatures in human colon epithelial cells

High-throughput and unbiased RNA sequencing was performed to evaluate the entire transcriptional program induced by SCFAs in Caco-2 cells. We observed 229 upregulated (pink dots) and eight downregulated (blue dots) top genes in acetate-treated cells (Fig. 6A). Propionate treatment resulted in more DEGs, including 72 downregulated and 665 upregulated genes (Fig. 6 B). Moreover, 636 downregulated and 2168 upregulated genes were observed in the butyrate-treated group (Fig. 6C), indicating that the lowest concentration of butyrate had a maximal impact on gene expression compared with the acetate- and propionate-treated groups. A Venn plot was used to define the expected gene expression modulations among the three treatments. A total of 198 signatures were disturbed in the three SCFA treatments (Fig. 6 D). Additionally, we identified one commonly changed gene between the acetate and butyrate groups, 24 commonly changed genes between the acetate and propionate groups, and 456 commonly changed genes between the propionate and butyrate groups. Signatures were defined based on criteria, including FDR-corrected $p < 0.001$ and an absolute fold change ≥ 4.

Pathways were significantly enriched in the SCFAs treatment compared with the control (Fig. 7), and heatmap analysis was used

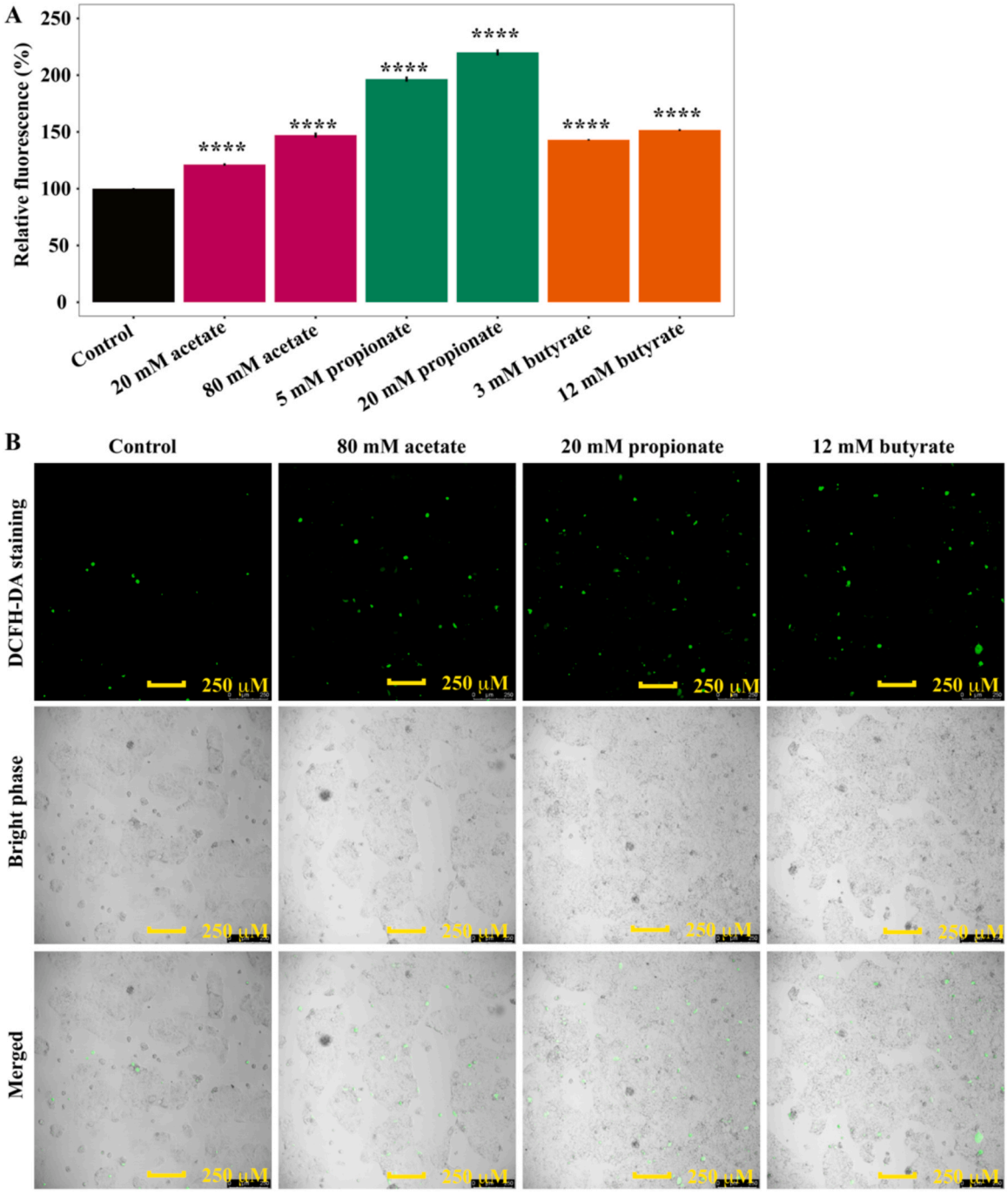

Fig. 2. Effects of different concentrations of SCFAs on ROS generation in Caco-2 cells. ROS production was detected by a DCFH-DA assay using a microplate reader (A) or laser confocal microscope (B, 10 × objective, scale bar =250 μM.) at 488 nm excitation and 525 nm emission. The statistical analysis was performed between the control and treatments using a one-way ANOVA with Dunnett's multiple comparisons test. * * * * represents $p < 0.0001$.

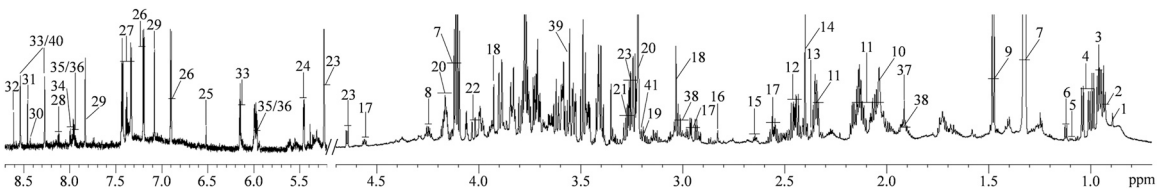

Fig. 3. Typical ^{1}H NMR spectra from the cell extracts of the control group. Key: 1, Pantothenate; 2, Isoleucine; 3, Leucine; 4, Valine; 5, α-keto-β -methyl-valerate; 6, α-Keto-isovalerate; 7, Lactic acid; 8, Threonine; 9, Alanine; 10, *N*-Acetyl-L-Glutamine; 11, Glutamate; 12, Glutamine; 13, Pyruvate; 14, Succinate; 15, Methionine; 16, Dimethylglycine; 17, Glutathione; 18, Creatine; 19, Choline; 20, Phosphocholine; 21, Taurine; 22, Fructose; 23, Glucose; 24, Galactose-1-phosphate; 25, Fumaric acid; 26, Tyrosine; 27, Phenylalanine; 28, Uridine 5′-monophosphate; 29, Histidine; 30, Nicotinamide adenine dinucleotide; 31, Formate; 32, Adenosine monophosphate; 33, Adenosine triphosphate; 34, Uridine 5′-diphosphate; 35, UDP Glucose; 36, UDP Glucuronate; 37, Acetate; 38, Lysine; 39, Glycine; 40, Adenosine diphosphate; 41, Acetylcholine.

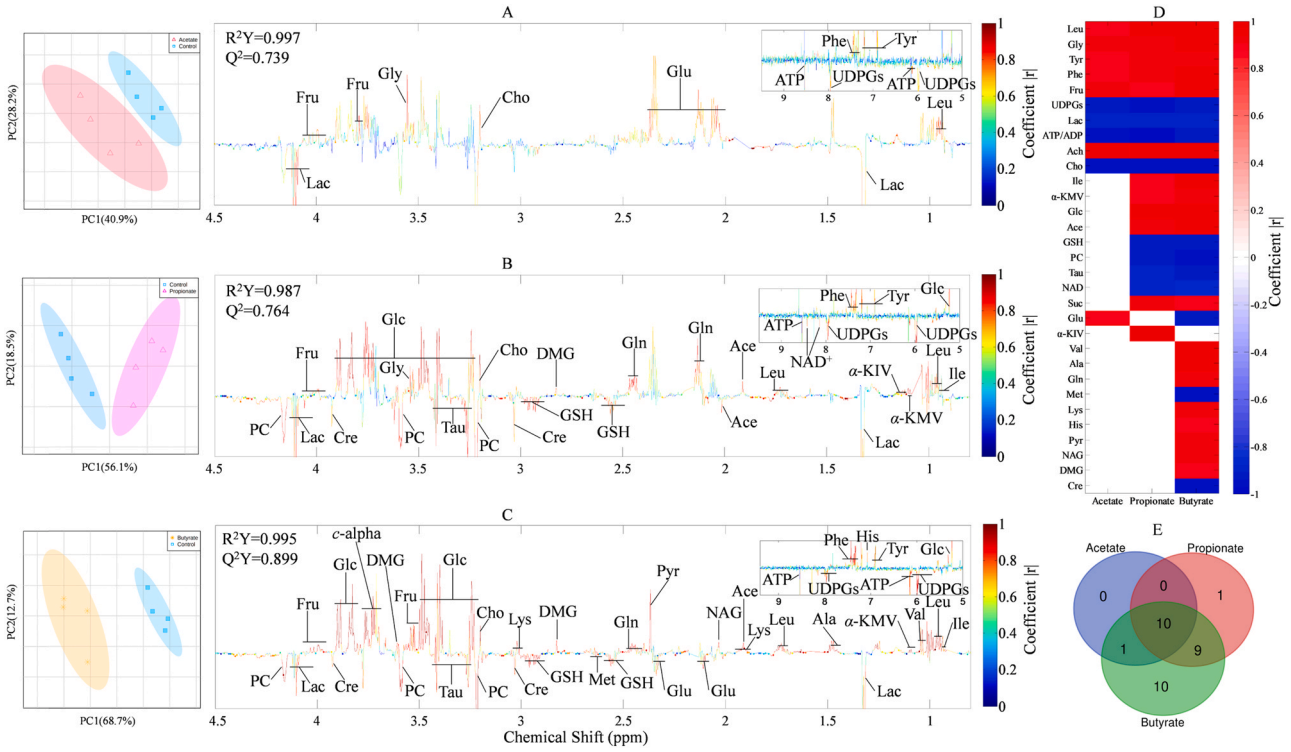

Fig. 4. Differential metabolomic profiles of the Caco-2 cells between the SCFAs-treated and control groups. A. PCA scores (left) of the complete metabolic profiles and color-coded correlation coefficient loadings plots generated by comparing the spectra of the intracellular metabolites between the acetate (A) and the control treatments; B. PCA scores (left) of the complete metabolic profiles and color-coded correlation coefficient loadings plots generated by comparing the spectra of the intracellular metabolites between the propionate (P) and the control treatments; C. PCA scores (left) of the complete metabolic profiles and color-coded correlation coefficient loadings plots generated by comparing the spectra of the intracellular metabolites between the butyrate (B) and the control treatments; D. Dynamic alterations of key metabolites in response to acetate, propionate and butyrate exposure. The color indicates a correlation coefficient as a scale on the right-hand side. Red denotes an increase in metabolite levels in the SCFAs-treated cells compared to the control group, whereas blue indicates a decrease; E, Venn diagram showing the number of metabolites that were changed in the Caco-2 cells in response to acetate, propionate, and butyrate treatment.

to define metabolism-related genes (Fig. 8). Thirty-two enriched pathways were identified and were mostly related to metabolic pathways, including upregulated pathways such as organic acid transport and catabolism, ROS metabolism, amino acid transport, and glutamine family amino acid catabolism, and downregulated pathways such as mitochondrial gene expression, oxidative phosphorylation, and amino acid activation and methylation. The extent of alteration in the expression of genes in these pathways gradually increased in the order of acetate, propionate, and butyrate (Fig. 8).

First, human colon cancer cells responded quickly to SCFAs treatment via the upregulation of the mRNA expression of solute carriers (SLCs, e.g., *SLC27A1*, *SCL2A4*, *SLC17A7,* and *SLC5A5*) (Fig. 8). Genes involved in mitochondrial transport and the respiratory chain complex, such as *MT.NDs*, *MT.CO1*, *MT.ATP6*, *COX10,* and *SIRT4* were significantly altered, suggesting that mitochondrial function was disturbed in SCFAs treated colon cells (Fig. 8). Meanwhile, the ROS response and metabolism were activated by elevated levels of *PLIN5*, *HVCN1*, *CDKN1A*, and *PREX1* and reduced levels of *IMMP2L* and *SIRT5* (Fig. 8). SCFAs treatment also significantly affected the expression of glucose import mRNAs (e.g., *ERFE*, *IGF1*, *INSR*, *RTN2*, *SLC27A1*, *ASPSCR1*, *SLC2A4,* and *IRS2*), polyol metabolic pathway (e.g., *ISYNA1*, *PCK1*, *SGPP1*, *IMPA1*, *DEGS2,* and *ASAH2*), glycolysis (e.g., *HKDC1*, *HK1*, *ENO2*, *PFKFB3*, and *PKM*), and pyruvate metabolism (e.g., *PPP1R1A*, *HK1,* and *PGM2L1*) (Fig. 8). One-carbon metabolism, comprising a series of interlinking metabolic pathways including the methionine and folate cycles and providing one carbon unit for the synthesis of DNA [37], showed significant elevations in the expression of *ALDH1L1*, *MBOAT2*, and *CA12* and reductions in the expression of *MTHFD2*, *MTHFS*, and *PCY1TB* (Fig. 8).

A previous report demonstrated that overexpression of most fatty acid transporters promotes CoA activity by two- to five-fold [38]. Consistently, our study also showed that SCFAs treatment resulted in significantly elevated expression of genes in the CoA-related pathway, including *HMGCLL1*, *HMGCS2*, *CPT1A* (β-oxidation), *ECI2*, *CRAT,* and *ACSF2* (Fig. 8).

3.6. Effects of SCFAs on gene expression detected by qRT-PCR

To validate the transcriptome data, qRT-PCR was used to determine the mRNA expression levels of the top 20 upregulated and downregulated genes in Caco-2 cells treated with low and high concentrations of SCFAs. The expression of *ANAX3, FOXQ1, MT-ATP6,* and *PITX1* mRNAs was downregulated at low concentrations of SCFAs compared to that in the control group (Fig. 9A), and their expression was more significantly suppressed in cells treated with high concentrations of SCFAs (Fig. 9B). Low concentrations of SCFAs had no effect on the mRNA levels for *CEBPD,* whereas the expression was significantly downregulated by high concentrations of SCFAs (Fig. 9). The mRNA levels of *CRIP2, EFNA3, ESAM, HK1, LGALS1, MCAM, NDRG4, NPAS1, NPPB, PHOSPHO1, SERPINI1, SLC16A3,* and *TUBB4A* were upregulated at low concentrations of SCFAs compared with those in the control group (Fig. 9A), and their expression was significantly increased with increasing concentrations of the treatment (Fig. 9B). Additionally, the expression of *ALPG* in acetate- and propionate-treated cells significantly increased at low and high SCFAs concentrations (Fig. 9). However, a high concentration of butyrate had no effect on *ALPG* expression, whereas a low concentration significantly enhanced *ALPG* expression (Fig. 9). Low concentrations

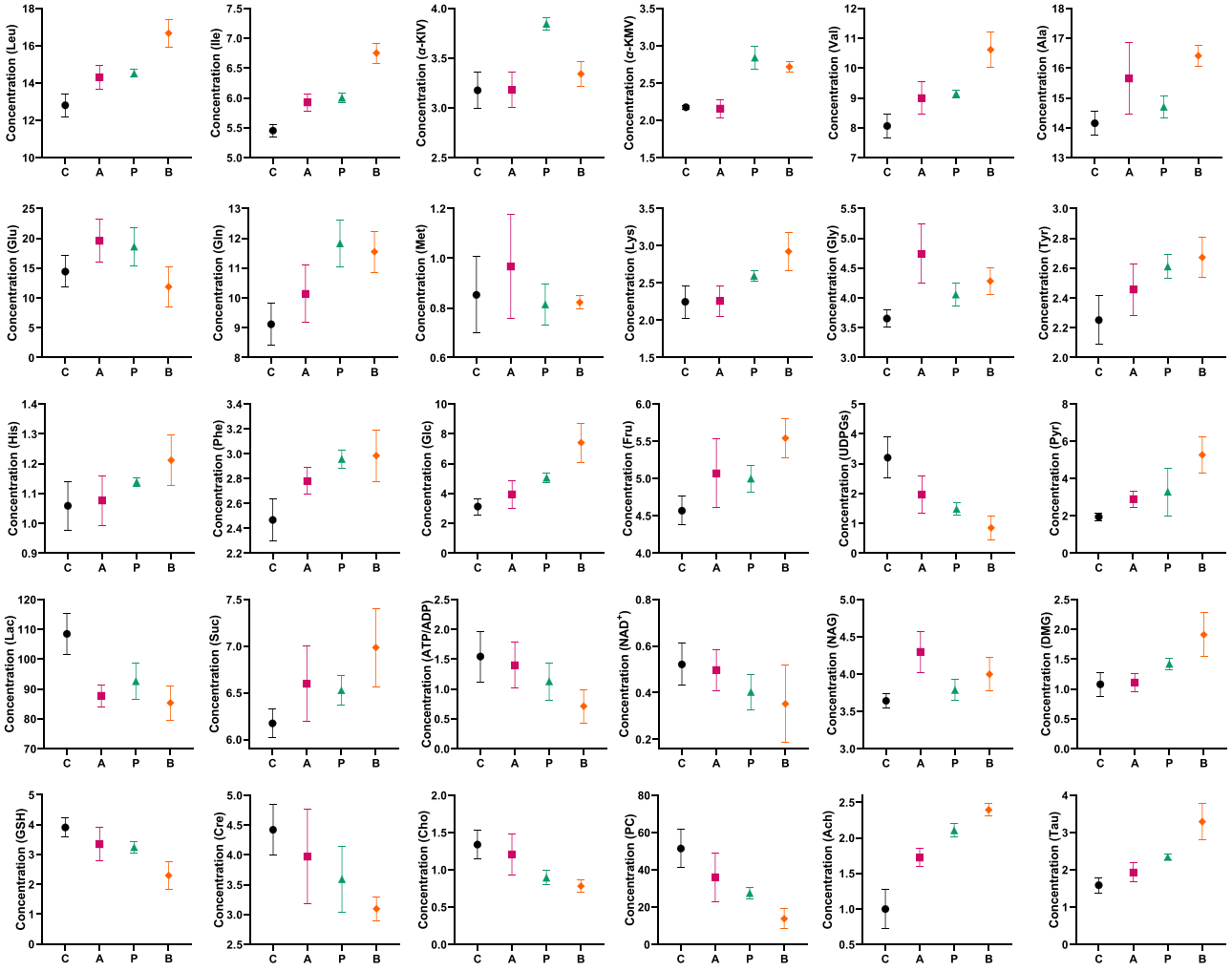

Fig. 5. Normalized concentrations of 32 significant change metabolites depending on the type of SCFAs. A: acetate; P: propionate; B: butyrate.

of SCFAs did not change the mRNA expression of *CDKN1A* compared to that in the control group, whereas high concentrations of propionate and butyrate significantly upregulated its expression (Fig. 9). Collectively, the qRT-PCR data were consistent with the RNA-seq data and showed that the regulation of SCFAs was dose-dependent in most genes. Fig. 10.

4. Discussion and Conclusions

Cancer is a genetic and metabolic disease [26]. Unlike most tissues that use glucose as their energy source, the colon utilizes SCFAs, particularly butyrate, as its primary energy source [39,40]. However, in most cancer cell lines, the primary energy metabolism pathway shifts from oxidative phosphorylation to glycolysis, which is a significant source of ATP synthesis [41]. Similarly, colorectal cancer cells shift their primary energy source from butyrate to glucose, resulting in increased glycolytic levels [42,43]. Several studies have shown that SCFAs suppress cancer progression by blocking glycolysis [10]. However, inconsistent viewpoints support the notion that butyrate is still the primary fuel for the human adenocarcinoma cell line HT-29 [44].

In contrast, SCFAs have been reported to alter the biology of cancer cells by inhibiting histone acetylation [45], suppressing cell proliferation [46], and inducing apoptosis [47]. Although research has been conducted on how SCFAs inhibit colon cancer cells, the molecular mechanisms remain unclear when considering the overall regulation of metabolic and transcriptomic profiles, owing to the complexity of intracellular molecular signaling pathways. In this study, we systematically analyzed the profiles of SCFA-induced disturbances at the metabolic and transcriptomic levels, which is critical for evaluating the mechanisms by which microbiota-derived metabolites regulate intestinal cancer by modulating the SCFAs ratio or concentration.

Moreover, 3 mM butyrate induced more severe disturbances at the metabolic and transcriptomic levels (Figs. 5 and 8), suggesting that Caco-2 cells responded more sensitively to butyrate exposure than to 20 mM acetate and 5 mM propionate. SCFAs significantly induced ROS production in Caco-2 cells in a concentration-dependent manner. Our RT-PCR data were consistent with RNA-seq data for 20 up/downregulated genes in cells treated with SCFAs at higher concentrations, and similar alterations were observed at low concentrations. Meanwhile, the metabolic analysis showed that 32 metabolites were disturbed and are involved in pathways including glucose uptake and metabolism, amino acid uptake and metabolism, choline uptake and metabolism, one-carbon metabolism, and mitochondrial respiratory function. Of these 32 metabolites, 21 showed dependence on the type of SCFAs, accompanied by corresponding transcriptomic changes acquired in the RNA sequence analysis. Subsequently, we discuss this issue in detail.

4.1. SCFAs modulated gene expression of transporter SLCs

First, exposure to SCFAs activated the expression of genes encoding membrane-bound transporter SLCs genes, which play vital

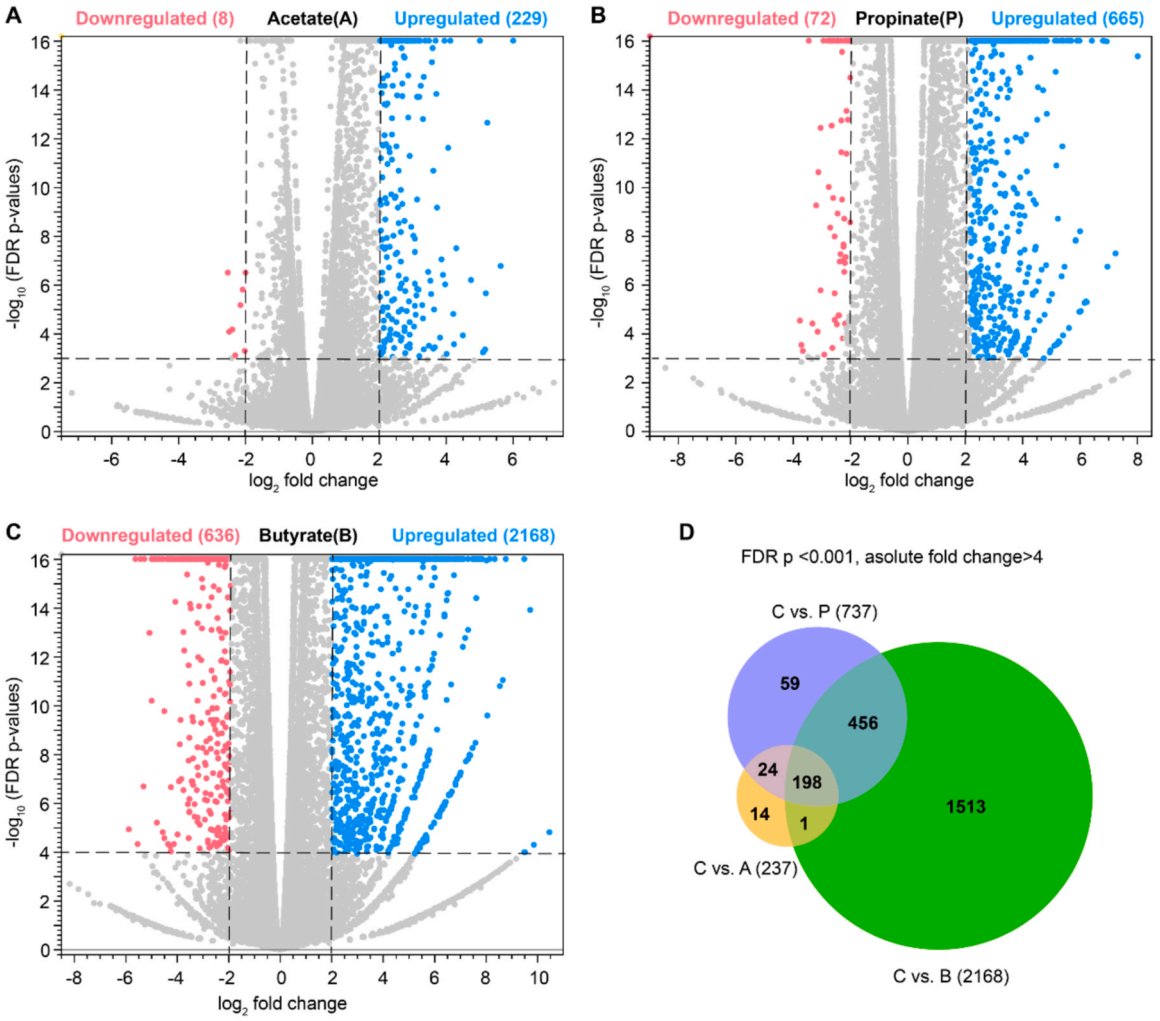

Fig. 6. Volcano plots showing the differentially expressed genes (DEGs) in the Caco-2 Cells responding to treatment with A, acetate, B, propionate, and C, butyrate compared to the control group; D, Venn diagram showing the number of mRNAs that changed in the Caco-2 cells in response to acetate, propionate, and butyrate treatment. FDR-corrected $p < 0.001$; absolute fold change > = 4. The blue dots represent the downregulated DEGs, and the red dots represent the upregulated DEGs. The gray dots represent the genes with no difference in expression.

roles in transporting substrates, including amino acids, glucose, other sugars, and fatty acids [48]. Particularly, we observed that *SLC27A1* (FATP), widely reported as a vital fatty acid transporter, was expressed at significantly higher levels in the SCFA-treated cells. Similar findings have been reported for the increased surface expression of *SLC27A1* in butyrate-treated HEK cells [49] and acetate-treated rabbit livers [50].

4.2. SCFAs induced mitochondria dysfunction

Dysfunctional mitochondria induce transcriptomic and metabolic disturbances [35]. Our results showed that SCFAs led to mitochondrial activity dysfunctions, such as the electron transport chain and oxidative phosphorylation and alterations in the expression of several genes related to mitochondrial function, such as decreased *MT-NDs*, *MT-CO1*, and *MT-ATP6* and increased *PIP5KL1*, *UCP1*, and *C15ORF48* (Fig. 8). Additionally, we observed increased succinate and decreased fumarate levels (although not significantly) in the SCFA-treated groups, a hallmark of electron transport chain dysfunction in complex II. Alterations of succinate dehydrogenase (*SDH)* complex genes involved in this pathway include increased *SDHA*, *SDHAF3*, and *SDHD* and decreased *SDHB*, *SDHC*, *SDHAF1*, *SDHAF2*, and *SDHAF3*.

4.3. SCFAs activated the ROS signaling pathway

Meanwhile, colon cancer cells with dysfunctional mitochondria that cannot efficiently metabolize SCFAs accumulate fatty acids in the cell [41] and increase cellular oxidative stress by elevating ROS production [39]. ROS, including hydroxyl radicals, superoxide anions, and hydrogen peroxide, formed during the single-electron reduction of molecular oxygen, modulate a few signaling pathways in the intestine and are recognized as central regulators of the function of intestinal stem cells [51]. Furthermore, ROS play a role in oxidizing and damaging proteins, lipids, and nucleic acids, and act as signaling molecules to activate self-protective mechanisms. In contrast, butyrate, propionate, and acetate treatments had decreased, no, or increased effects on ROS production in rat neutrophils [52]. Maslowski et al. discovered that acetate promoted the release of ROS when added to mouse neutrophils by activating GPR43 [53]. Researchers in the field of immunology consider that SCFAs may regulate inflammatory diseases by accelerating pathogen clearance via ROS activation [54]. SCFAs have been reported to suppress cancer progression by increasing ROS levels. For example, sodium butyrate induces apoptosis following an increase in ROS levels in breast cancer cells [55]. Additionally, butyrate increases ROS levels in colorectal cancer cells and inhibits cell proliferation [56] by regulating

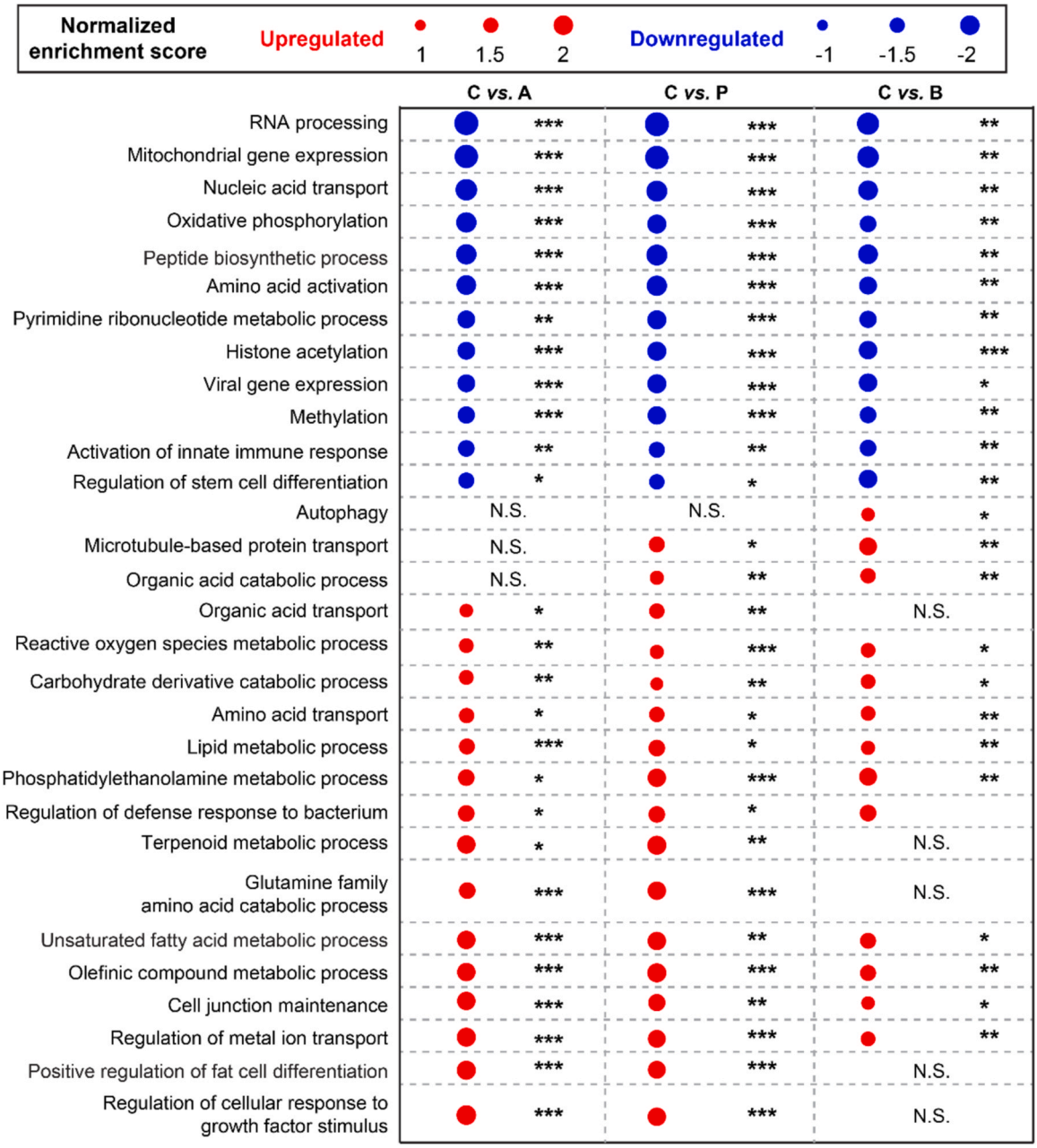

Fig. 7. Pathways were significantly enriched in SCFAs-treatment compared with controls. Negative normalized enrichment scores (blue dots) show downregulated pathways and positive normalized enrichment scores (red dots) show upregulated pathways. * Adjusted $p < 0.05$, * * Adjusted $p < 0.01$, * * *Adjusted $p < 0.001$. A: acetate; P: propionate; B: butyrate.

the expression of the histone deacetylase SIRT-1 [57]. Another study demonstrated that butyrate induces apoptosis through the upregulation of miR-22, followed by the downregulation of *SIRT-1*, resulting in increased ROS production and apoptosis of hepatic cells. This study has shown significantly higher levels of ROS in the three types of SCFA treatments at physiological concentrations in Caco-2 cells. SCFAs significantly altered the expression of genes involved in ROS production, such as *PLIN5* [58], *CDKN1A* [59], *PREX1* [60], *UCP1* [59], *FYN* [61], *COLIA1* [62], *FOXO1* [63], *IMMP2L* [64], and *DUOXA2* [65]. These results suggest that SCFAs activate ROS signaling pathways via the modulation of metabolic and transcriptomic signatures.

Sirtuins (SIRT) regulate the energy state of cells, which is associated with oxidative stress signaling and antioxidant defense in the cells [66]. We observed elevated *SIRT4* and *SIRT2* expression and reduced expression of *SIRT5* in SCFA-treated cells. *SIRT2* is mainly localized in the cytoplasm [67], whereas *SIRT4* and *SIRT5* are localized in the mitochondria [67,68]. SIRT4 plays a vital role in suppressing tumor progression by regulating glutamine metabolism. The overexpression and knockout of *SIRT4* [69] showed elevated and reduced ROS levels, respectively. *SIRT5* has been associated with reprogramming metabolic pathways, including glycolysis, the TCA cycle, and electron transport chain [70], which promotes tumor cell metabolism. Lu et al. reported that SIRT5 facilitates cell growth in non-small cell lung cancer [71]. SIRT5 facilitates the consumption of ammonia [72], which is vital for inducing ROS production and decreasing the levels of the antioxidant GSH [73]. In this study, increased ROS and decreased GSH levels were consistently observed. Cancer cells are more tolerant to oxidative stress than normal cells and have a higher capacity to scavenge ROS to increase their survival rate [74]. GSH improves antioxidant capacity and resistance to

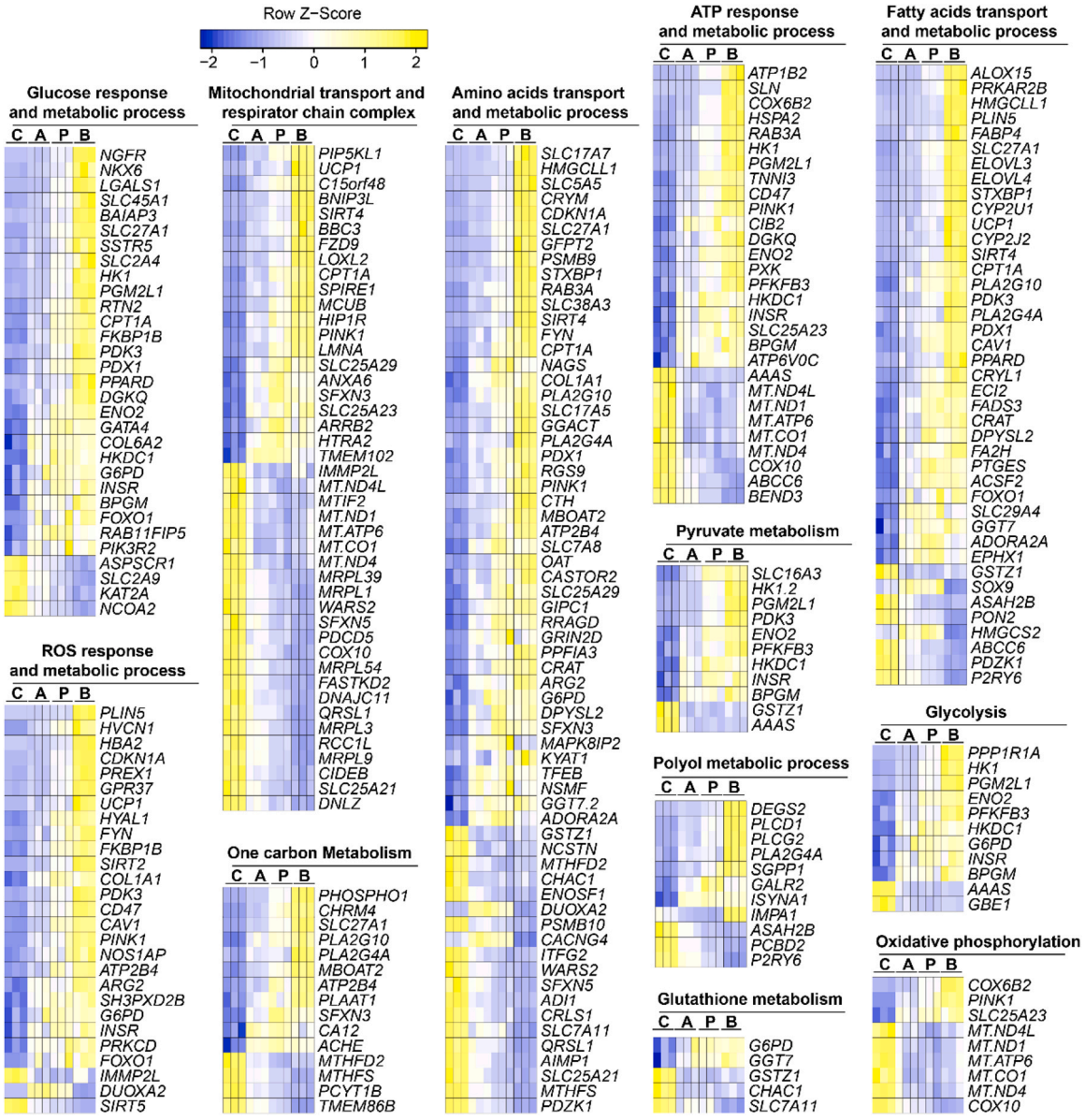

Fig. 8. Supervised heat maps of differentially expressed genes in all SCFAs-treated cells in the enriched gene sets. The enriched gene sets were analyzed using supervised hierarchical clustering in Heatmapper including DEGs with an FDR-corrected $p < 0.05$ and fold change ≥ 1.5, upregulated (red) genes, and downregulated (green) genes in the SCFAs treatment vs. the control groups. A: acetate; P: propionate; B: butyrate.

oxidative stress in cancer cells [75]. Low GSH levels have been observed to increase the sensitivity of cancer cell lines to irradiation [76]. GSH is vital for maintaining the intracellular redox state and regulating the sensitivity of cancer cells to apoptosis [55,77]. Several studies have reported the depletion of GSH by butyrate exposure in various cell lines, including Caco-2 [78,79], MCF-7 [80], and HT29 [81,82].

4.4. One-carbon Metabolism Pathway was reprogrammed by SCFAs treatment

The trans-sulfuration pathway synthesizes GSH and is involved in ROS production in cancer cells [83]. The low levels of GSH in this study indicated that treatment with SCFAs might alter the trans-sulfuration pathway, one of the three critical reactions of the one-carbon metabolic pathway. One-carbon metabolism serves as a vital modulation pathway [84] and is present in both the mitochondria and cytoplasm of cancer cells. As another reaction involved in one-carbon metabolism, the folate cycle is vital for purine production and serine is a necessary metabolite. This process converts serine to glycine by serine hydroxymethyl transferases 1 and 2 (SHMT1 and SHMT2) in the cytosol and mitochondria, respectively [85]. However, we could not detect any disturbance in the metabolic levels of serine because of its limited physiological concentration. However, only *SHMT2* in the mitochondria and not *SHMT1* in the cytosol was significantly decreased in all three SCFA-treated groups. Additionally, significantly reduced levels of *SHMT1* were detected only in the acetate-treated cells.

Sideroflexin (*SFXN1–5)* is a mitochondrial transporter of serine in one-carbon metabolism, and *SFXN1* and *SFXN*3 play essential roles in maintaining glycine balance [86]. This study demonstrated that SCFAs significantly decreased *SFXN1*, *SFXN2*, *SFXN4*, and *SFXN5* but increased *SFXN3* expression, indicating that SCFAs modulated the serine transporter pathway. However, interpreting underlying mechanisms is challenging. Additionally, we observed significantly increased glycine levels in all the SCFA-treated cells; however, glycine

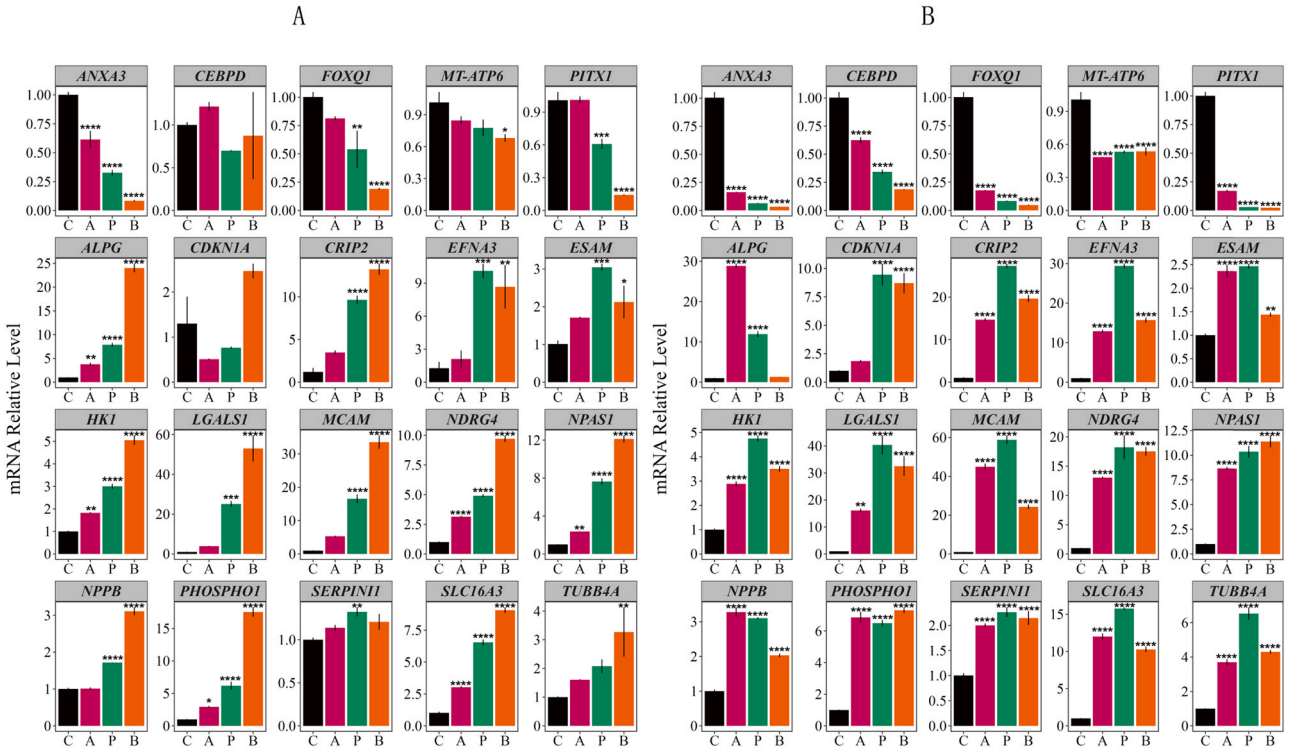

Fig. 9. mRNA expression in Caco-2 cells treated with SCFAs of low (A) or high (B) concentration. Data are expressed as mean ± SD (n = 4). The statistical analysis was performed between the control and treatments using one-way ANOVA with Dunnett's multiple comparisons test. ** represents $p < 0.01$, *** represents $p < 0.001$, and **** represents $p < 0.0001$. A: acetate; P: propionate; B: butyrate.

insufficiency has been reported in studies involving cells lacking mitochondrial components [87–89]. Moreover, protein kinase C (PKC) activation has been reported to reduce the expression of *GLYT1* in Caco-2 cells with high levels of glycine [90]. Consistently, the glycine transporter gene *GLYT1* (*SLC6A9*) was significantly reduced and *PRKCD*, a member of the novel PKC subfamily, was upregulated in this study. Taken together, these results suggest that glycine levels in cells may be elevated via other pathways. Considering that supplementary glycine has been reported to prevent cancer [91], we speculated that SCFAs effectively inhibit cancer progression by, at least in part, upregulating glycine levels.

4.5. Different types of SCFAs resulted in different profiles of glutaminolysis pathway

The myelocytomatosis oncogene (*MYC*) plays an essential role in glutamine metabolism [92] by activating glutamine transporters *SLC1A5* and *SLC38A5* [93] and enhancing glutaminolysis by elevating glutaminase (GLS) translation [94]. We observed significantly elevated levels of glutamine in propionate- and butyrate-treated cells but did not observe a significant variance in the acetate treatment group. However, glutamate, the downstream metabolite of glutamine, significantly decreased in the butyrate group and increased in the acetate group. Increased glutamate levels were also observed in the propionate treatment group, although the difference was not significant.

MYC, which regulates the activities of GLS, showed a similar expression profile to glutamate, with increased expression in acetate- and propionate-treated cells and decreased expression in the butyrate-treated group. These results indicated that SCFAs induced disturbances of glutaminolysis in Caco-2 cells in a specific manner, depending on the type of SCFAs.

4.6. SCFAs caused alterations in glucose metabolism

In addition to regulating glutamine metabolism, MYC modulates aerobic glycolysis by promoting glucose uptake (by enhancing glucose transporter *SLC2A1* expression [95]), activating the production of pyruvate (by elevating PKM expression [96]), and modulating lactate export (by inducing lactate transporters-monocarboxylate transporters MCT1 and MCT2 [97]). First, butyrate treatment increases glucose uptake in Caco-2 cells [98]. In this study, we also observed elevated glucose and altered expression of *GLUT* genes in SCFA-treated Caco-2 cell lines, including increased insulin-regulated gene *GLUT4* (*SLC2A4*) and decreased expression of non-insulin-dependent genes *GLUT2* (*SLC2A2*) and *GLUT9* (*SLC2A9*), which is in contrast with previous reports on increased gene expression of *GLUT2* in SCFA-treated cells [99,100]. Meanwhile, the metabolic analysis showed that elevated glucose levels were induced by SCFAs exposure, which is consistent with a previous study and indicated that increased glucose uptake in colon cancer cells could lead to oxidative phosphorylation damage through lactate-induced mitochondrial dysfunction [101].

Pyruvate dehydrogenase kinase (PDK) is a regulatory enzyme of the pyruvate dehydrogenase complex (PDC) that serves as a crossroad between glycolysis and the tricarboxylic acid cycle [102]. Elevated *PDK1–4* expression was detected in the propionate- and butyrate-treated groups, while elevated *PDK2–3* expression was observed in the acetate group. Higher levels of pyruvate were observed in the SCFA-treated group, although this was statistically significant only in butyrate-treated cells. PDK is an inhibitor of PDC, suggesting that pyruvate was blocked in the TCA cycle and might accumulate in the mitochondria, where elevated levels of PDK inhibited the activity of PDC.

Lactate is the end product of glycolysis and is essential for cancer progression. Butyrate induced a lower level of lactate in a

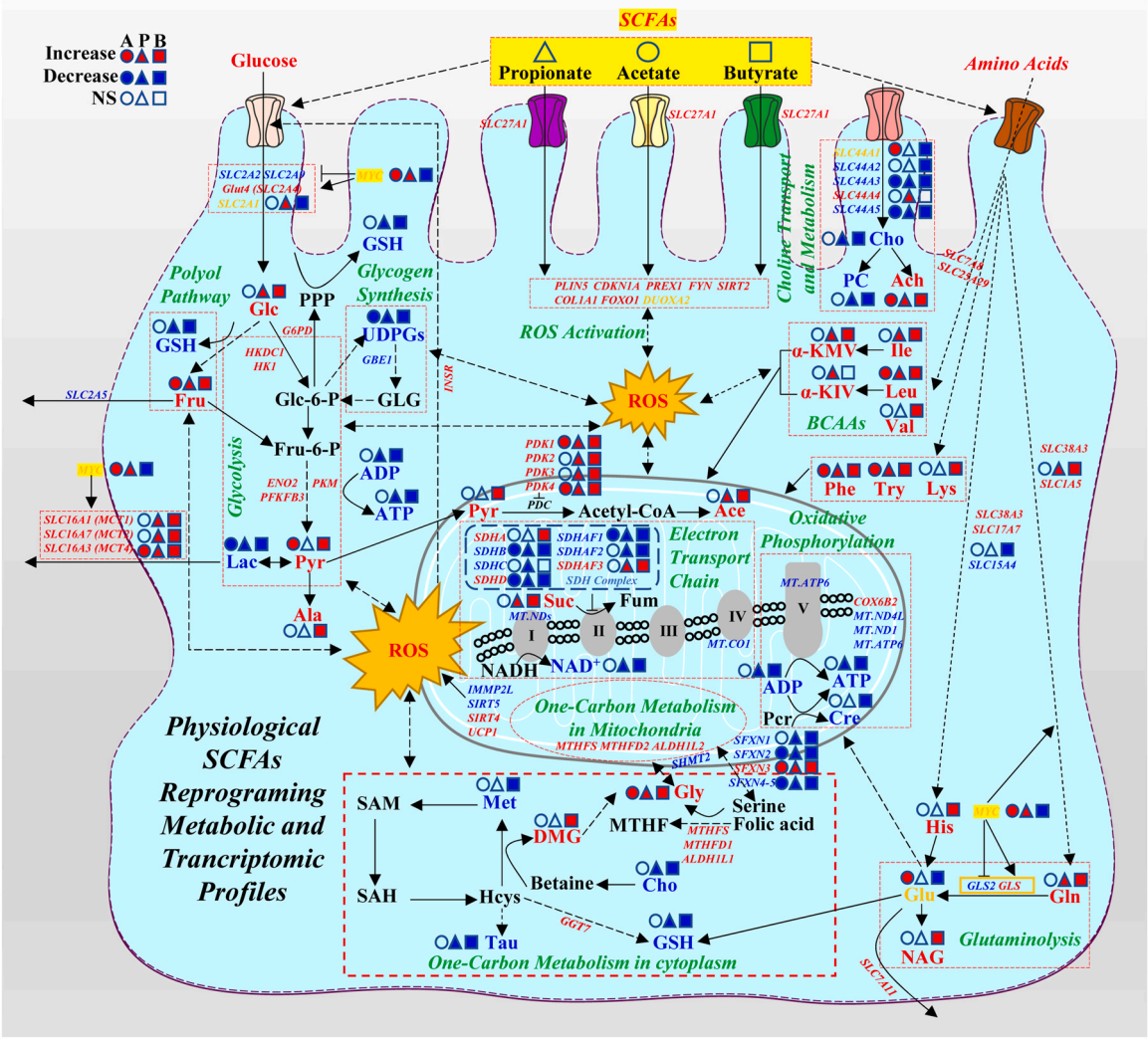

Fig. 10. Metabolic and transcriptomic alterations of pathways under SCFAs exposure. Blue, red, and orange indicate the downregulated, upregulated and up/down-regulated pathways, respectively. A: acetate; P: propionate; B: butyrate.

remarkably enriched source of pyruvate in HCT116 cells and was used as an indicator of a metabolic shift from anabolic processes, which are vital for tumor cell proliferation, oxidative phosphorylation, and energy production [46]. Consistently, significantly lower lactate levels were observed in all the SCFA-treated cells in the present study. However, the *LDH* gene expression was not disturbed. These results suggested that lower lactate levels may not be caused by elevated pyruvate levels. Furthermore, a higher expression level of the lactate transporter *SLC16A3* (MCT4) was observed in the SCFA-treated cells. MCT4 may be particularly appropriate for the export of lactate derived from glycolysis [103]. Additionally, the levels of other mRNAs related to lactate transporters, including *SLC16A1* (MCT1) and *SLC16A7* (MCT2), were increased in propionate- and butyrate-treated cancer cells. Our data indicate that reduced lactate levels might be due to the increased activity of lactate transporters.

The level of fructose was increased by SCFAs through the polyol pathway in Caco-2 cells, accompanied by a decrease in the fructose transporter gene *GLUT5* (*SLC2A5*). Elevated levels of *GLUT5* are associated with poor prognosis in patients with lung adenocarcinoma, and depletion of *GLUT5* inhibits cell proliferation and invasion and increases apoptosis [104]. Moreover, high expression of *GLUT5* and enhanced fructose utilization are associated with poor outcomes and exacerbate leukemic phenotypes [105]. Moreover, the polyol process is accompanied by the oxidation of NADPH to $NADP^+$, which causes GSH deficiency, because NADPH is necessary to produce GSH from GSSG [106]. However, the oxidative pentose phosphate pathway (PPP), the primary provider of NADPH for GSH synthesis, has been reported to be activated by SCFAs in the Kato 3 gastric cancer cell line [55]. Our study showed that the expression of G6PD, a rate-limiting enzyme that catalyzes the first step of PPP, is activated by SCFAs. Elevated oxidative PPP was linked to an increase in the oxidative state, which might induce ROS production. In our study, despite elevated ROS and decreased GSH levels involved in the PPP pathway, no significant changes in metabolites were detected, indicating that the level of GSH may be modulated in SCFA-treated cancer cells. Additionally, the glycogen synthesis pathway may be inhibited because decreased levels of *GBE1 and UDPGs* involved *in* glycogen synthesis were observed in SCFA-treated cells.

4.7. SCFAs induced disturbances in the choline transport and metabolism

Increased choline and phosphocholine levels have been observed in cancer cells from the brain, breast, prostate, and colon [107]. In this study, exposure to SCFAs induced a wide range of disturbances in choline transport and metabolic pathways. This study showed significantly altered expression of the transporter gene, *SLC44A1–5*, and choline metabolism, including elevated acetylcholine and

decreased choline and PC. A review of this process indicated that cells would elevate phospholipid generation and promote apoptosis when choline is restricted to transport into the cell [107]. We speculate that SCFAs induce cancer cell death, at least partly through the modulation of choline transport.

4.8. SCFAs altered the transport and metabolism of amino acids

Amino acids were significantly elevated in SCFA-treated cells, accompanied by an increased expression of amino acid transporters, indicating that SCFAs promoted amino acid uptake. We observed several increased levels of amino acids, including leucine, isoleucine, valine, lysine, phenylalanine, and tyrosine, in SCFA-treated cells. In addition, glutamine serves as an energy source and helps maintain the redox balance. Branched-chain amino acids such as valine, leucine, and isoleucine can fuel the TCA cycle [108] as alternative sources, contributing to bioenergetic pathways [108], mediating lipogenesis, and regulating nucleotide synthesis [109]. Nonetheless, further detailed studies are required to investigate the mechanisms underlying these alterations.

In this study, we combined metabolomics and transcriptomics to determine how SCFAs regulate cell metabolism and transcriptomes by producing high levels of ROS. However, endogenous metabolic changes result from comprehensive and complex cellular regulatory processes. A typical example in this study is the final level of GSH, which is regulated by multiple pathways, including the polyol pathway, PPP, one-carbon metabolism pathway, glutaminolysis pathway, and unidentified pathways. Further studies are warranted to determine the precise metabolic flux of one or more metabolites using dissolution dynamic nuclear polarization (dDNP) [110], which is a robust tool for studying real-time metabolic flux. Particularly, whether SCFAs regulate metabolic pathways via ROS activation remains an important question, or whether these effects represent indirect consequences of mitochondrial and cellular physiology changes. Additionally, it is worth studying the combined effects of SCFAs, because they are not present individually in the human colon as the sole metabolites.

Funding

This project was funded by Wuhan Botanical Garden, Chinese Academy of Sciences, China, grant No. E2559901; National Major Scientific Research Equipment Development Project of China, Grant/Award Numbers: 81627901; National Major Scientific Research Equipment Development Project of China, Grant/Award Numbers: 21927801; National Major Scientific Research Equipment Development Project of China, Grant/Award Numbers: 22127801.

CRediT authorship contribution statement

Conceptualization, **Jing Li**, **Chaoyang Liu** and **Chongyang Huang**; investigation, **Chongyang Huang**, **Wenjun Deng**, **Huanzhou Xu**; **Chen Zhou**, **Fan Zhang**; writing, **Chongyang Huang**; writing (review and edit), **Chongyang Huang**, **Wenjun Deng**, **Huanzhou Xu**, **Junfei Chen**, **Qinjia Bao**, **Xin Zhou**, **Maili Liu**, **Jing Li** and **Chaoyang Liu**; supervision, **Chaoyang Liu** and **Jing Li**. All authors have read and agreed to the published version of the manuscript.

Declaration of Competing Interest

The authors declare that they have no known competing financial interests or personal relationships that could have appeared to influence the work reported in this paper.

Acknowledgments

The authors would like to thank members of their lab for helpful and constructive advice.

Appendix A. Supporting information

Supplementary data associated with this article can be found in the online version at doi:10.1016/j.csbj.2023.02.022.

References

[1] Dinan, T.; Stilling, R.; Stanton, C.; Cryan, J.; Dinan, T.G.; Stilling, R.M.; Cryan, J.F., Collective unconcious: how gut microbes shape human behaviour. 2015.
[2] Anwar H, Irfan S, Hussain G, Faisal MN, Ullah MI. Gut microbiome: a new organ system in body. Eukaryot Microbiol 2019.
[3] Tang Y, Chen Y, Jiang H, Nie D. The role of short-chain fatty acids in orchestrating two types of programmed cell death in colon cancer. Autophagy 2011;7(2):235–7.
[4] Van d B, Bloemen CM, Van JG, M. A d B, Lenaerts K, Venema K, Buurman WA, Dejong CH. Hepatic uptake of rectally administered butyrate prevents an increase in systemic butyrate concentrations in humans. J Nutr 2015;145(9):2019–24.
[5] Cummings H, J. Short chain fatty acids in the human colon. Gut 1981;22(9):763–79.
[6] Silva YP, Bernardi A, Frozza RL. The role of short-chain fatty acids from gut microbiota in gut-brain communication. Front Endocrinol 2020:*11*.
[7] Ohigashi S, Sudo K, Kobayashi D, Takahashi T, Nomoto K, Onodera H. Significant changes in the intestinal environment after surgery in patients with colorectal cancer. J Gastrointest Surg 2013;17(9):1657–64.
[8] Microbial butyrate and its role for barrier function in the gastrointestinal tract. Ann N Y Acad ences 2012;1258(1).
[9] Wells Jerry, Rossi M, Meijerink Oriana, Marjolein van, Baarlena Peter. Epithelial crosstalk at the microbiota– mucosal interface. *Proc Natl Acad Sci USA* 2011;108:4607–14. (Supplement_1).
[10] Geng HW, Yin FY, Zhang ZF, Gong X, Yang Y. Butyrate suppresses glucose metabolism of colorectal cancer cells via GPR109a-AKT signaling pathway and enhances chemotherapy. Front Mol Biosci 2021;8:634874.
[11] Eugene Oltz, Koues M, Olivia I, Edward Pearce, Solnica-Krezel J. The colonic crypt protects stem cells from microbiota-derived metabolites. (Vol 165, pg 1708, 2016) *Cell* 2016;167(4). 1137-1137.
[12] Hee B, Wells JM. Microbial regulation of host physiology by short-chain fatty acids. Trends Microbiol 2021;29(8).
[13] Portincasa P, Bonfrate L, Vacca M, De Angelis M, Farella I, Lanza E, Khalil M, Wang DQ, Sperandio M, Di Ciaula A. Gut microbiota and short chain fatty acids: implications in glucose homeostasis. Int J Mol Sci 2022;23:3.
[14] Venegas DP, Fuente M, Landskron G, González M, Hermoso MA. Short chain fatty acids (SCFAs)-Mediated gut epithelial and immune regulation and its relevance for inflammatory bowel diseases. Front Immunol 2019;10:277.
[15] Brody LP, Sahuri-Arisoylu M, Parkinson JR, Parkes HG, So PW, Hajji N, Thomas EL, Frost GS, Miller AD, Bell JD. Cationic lipid-based nanoparticles mediate functional delivery of acetate to tumor cells in vivo leading to significant anticancer effects. Int J Nanomed 2017;12:6677–85.
[16] Lan A, Lagadic-Gossmann D, Lemaire C, Brenner C, Jan G. Acidic extracellular pH shifts colorectal cancer cell death from apoptosis to necrosis upon exposure to propionate and acetate, major end-products of the human probiotic propionibacteria. Apoptosis 2007;12(3):573–91.
[17] Sahuri-Arisoylu M, Mould RR, Shinjyo N, Bligh SWA, Nunn AVW, Guy GW, Thomas EL, Bell JD. Acetate induces growth arrest in colon cancer cells through modulation of mitochondrial function. Front Nutr 2021;8:588466.
[18] Ryu TY, Kim K, Han TS, Lee MO, Lee J, Choi J, Jung KB, Jeong EJ, An DM, Jung CR, Lim JH, Jung J, Park K, Lee MS, Kim MY, Oh SJ, Hur K, Hamamoto R, Park DS, Kim DS, Son MY, Cho HS. Human gut-microbiome-derived propionate coordinates proteasomal degradation via HECTD2 upregulation to target EHMT2 in colorectal cancer. Isme J 2022;16(5):1205–21.
[19] Matthews GM, Howarth GS, Butler RN. Short-chain fatty acids induce apoptosis in colon cancer cells associated with changes to intracellular redox state and glucose metabolism. Chemotherapy 2012;58(2):102–9.
[20] Zeng H, Hamlin SK, Safratowich BD, Cheng WH, Johnson LK. Superior inhibitory efficacy of butyrate over propionate and acetate against human colon cancer cell proliferation via cell cycle arrest and apoptosis: linking dietary fiber to cancer prevention. Nutr Res 2020;83:63–72.
[21] Elamin EE, Masclee AA, Dekker J, Pieters HJ, Jonkers DM. Short-chain fatty acids activate AMP-activated protein kinase and ameliorate ethanol-induced intestinal barrier dysfunction in Caco-2 cell monolayers. J Nutr 2013;143(12):1872–81.
[22] Suzuki T, Yoshida S, Hara H. Physiological concentrations of short-chain fatty acids immediately suppress colonic epithelial permeability. Br J Nutr 2008;100(2):297–305.
[23] Mariadason JM, Barkla DH, Gibson PR. Effect of short-chain fatty acids on paracellular permeability in Caco-2 intestinal epithelium model. *Am J Physiol* 1997;272(4 Pt 1):G705–12.

[24] DeSoignie R, Sellin JH. Propionate-initiated changes in intracellular pH in rabbit colonocytes. Gastroenterology 1994;107(2):347–56.
[25] Morgan TR, Mandayam S, Jamal MM. Alcohol and hepatocellular carcinoma. Gastroenterology 2004;127(5 Suppl 1):S87–96.
[26] Wang K, Jiang J, Lei Y, Zhou S, Wei Y, Huang C. Targeting metabolic-redox circuits for cancer therapy. Trends Biochem Sci 2019;44(5):401–14.
[27] Luo Y, Geng N, Zhang B, Chen J, Zhang H. Effects of harvesting and extraction methods on metabolite recovery from adherently growing mammalian cells. Anal Methods 2020;12(19):2491–8.
[28] Beckonert O, Keun HC, Ebbels TM, Bundy J, Holmes E, Lindon JC, Nicholson JK. Metabolic profiling, metabolomic and metabonomic procedures for NMR spectroscopy of urine, plasma, serum and tissue extracts. Nat Protoc 2007;2(11):2692.
[29] Pang Z, Chong J, Zhou G, de Lima Morais DA, Chang L, Barrette M, Gauthier C, Jacques P-É, Li S, Xia J. MetaboAnalyst 5.0: narrowing the gap between raw spectra and functional insights. Nucleic Acids Res 2021;49(W1):W388–96.
[30] Cloarec O, Dumas ME, Trygg J, Craig A, Barton RH, Lindon JC, Nicholson JK, Holmes E. Evaluation of the orthogonal projection on latent structure model limitations caused by chemical shift variability and improved visualization of biomarker changes in 1H NMR spectroscopic metabonomic studies. Anal Chem 2005;77(2):517–26.
[31] Korotkevich G, Sukhov V, Budin N, Shpak B, Artyomov MN, Sergushichev A. Fast gene set enrichment analysis. BioRxiv 2021:060012.
[32] Babicki S, Arndt D, Marcu A, Liang Y, Grant JR, Maciejewski A, Wishart DS. Heatmapper: web-enabled heat mapping for all. Nucleic Acids Res 2016;44(W1):W147–53.
[33] Schug ZT, Voorde Vande, Gottlieb J. E., The metabolic fate of acetate in cancer. Nat Rev Cancer 2016;16(11):708–17.
[34] Parada Venegas D, De la Fuente MK, Landskron G, González MJ, Quera R, Dijkstra G, Harmsen HJM, Faber KN, Hermoso MA. Short Chain Fatty Acids (SCFAs)-Mediated Gut Epithelial and Immune Regulation and Its Relevance for Inflammatory Bowel Diseases. Front Immunol 2019;10:277.
[35] Huang C, Xu H, Zhou X, Liu M, Li J, Liu C. Systematic investigations on the metabolic and transcriptomic regulation of lactate in the human colon epithelial cells. Int J Mol Sci 2022;23(11).
[36] Kostidis S, Addie RD, Morreau H, Mayboroda OA, Giera M. Quantitative NMR analysis of intra- and extracellular metabolism of mammalian cells: A tutorial. Anal Chim Acta 2017;980:1–24.
[37] Clare CE, Brassington AH, Kwong WY, Sinclair KD. One-carbon metabolism: linking nutritional biochemistry to epigenetic programming of long-term development. Annu Rev Anim Biosci 2019;7:263–87.
[38] Daniel H. Molecular physiology of plasma membrane transporters for organic nutrients. Mol Nutr 2003:90.
[39] Ganapathy V, Thangaraju M, Prasad PD, Martin PM, Singh N. Transporters and receptors for short-chain fatty acids as the molecular link between colonic bacteria and the host. Curr Opin Pharm 2013;13(6):869–74.
[40] Rivière A, Selak M, Lantin D, Leroy F, De Vuyst L. Bifidobacteria and Butyrate-Producing Colon Bacteria: Importance and Strategies for Their Stimulation in the Human Gut. Front Microbiol 2016;7:979.
[41] Zheng J. Energy metabolism of cancer: Glycolysis versus oxidative phosphorylation (Review). Oncol Lett 2012;4(6):1151–7.
[42] do Prado SBR, Castro-Alves VC, Ferreira GF, Fabi JP. Ingestion of non-digestible carbohydrates from plant-source foods and decreased risk of colorectal cancer: a review on the biological effects and the mechanisms of action. Front Nutr 2019;6:72.
[43] den Besten G, Lange K, Havinga R, van Dijk TH, Gerding A, van Eunen K, Müller M, Groen AK, Hooiveld GJ, Bakker BM, Reijngoud DJ. Gut-derived short-chain fatty acids are vividly assimilated into host carbohydrates and lipids. Am J Physiol Gastrointest Liver Physiol 2013;305(12):G900–10.
[44] Leschelle X, Delpal S, Goubern M, Blottière HM, Blachier F. Butyrate metabolism upstream and downstream acetyl-CoA synthesis and growth control of human colon carcinoma cells. Eur J Biochem 2000;267(21):6435–42.
[45] Li Q, Ding C, Meng T, Lu W, Liu W, Hao H, Cao L. Butyrate suppresses motility of colorectal cancer cells via deactivating Akt/ERK signaling in histone deacetylase dependent manner. J Pharm Sci 2017;135(4):148–55.
[46] Li Q, Cao L, Tian Y, Zhang P, Ding C, Lu W, Jia C, Shao C, Liu W, Wang D, Ye H, Hao H. Butyrate suppresses the proliferation of colorectal cancer cells via targeting pyruvate kinase m2 and metabolic reprogramming. Mol Cell Proteom 2018;17(8):1531–45.
[47] Xu S, Liu CX, Xu W, Huang L, Zhao JY, Zhao SM. Butyrate induces apoptosis by activating PDC and inhibiting complex I through SIRT3 inactivation. Signal Transduct Target Ther 2017;2:16035.
[48] He L, Vasiliou K, Nebert DW. Analysis and update of the human solute carrier (SLC) gene superfamily. Hum Genom 2009;3(2):195–206.
[49] Trompette A, Pernot J, Perdijk O, Alqahtani RAA, Domingo JS, Camacho-Muñoz D, Wong NC, Kendall AC, Wiederkehr A, Nicod LP, Nicolaou A, von Garnier C, Ubags NDJ, Marsland BJ. Gut-derived short-chain fatty acids modulate skin barrier integrity by promoting keratinocyte metabolism and differentiation. Mucosal Immunol 2022;15(5):908–26.
[50] Fu C, Liu L, Li F. Acetate alters the process of lipid metabolism in rabbits. Animal 2018;12(9):1895–902.
[51] Morris O, Jasper H. Reactive Oxygen Species in intestinal stem cell metabolism, fate and function. Free Radic Biol Med 2021;166:140–6.
[52] Vinolo MA, Hatanaka E, Lambertucci RH, Newsholme P, Curi R. Effects of short chain fatty acids on effector mechanisms of neutrophils. Cell Biochem Funct 2009;27(1):48–55.
[53] Maslowski KM, Vieira AT, Ng A, Kranich J, Sierro F, Yu D, Schilter HC, Rolph MS, Mackay F, Artis D, Xavier RJ, Teixeira MM, Mackay CR. Regulation of inflammatory responses by gut microbiota and chemoattractant receptor GPR43. Nature 2009;461(7268):1282–6.
[54] Tan J, McKenzie C, Potamitis M, Thorburn AN, Mackay CR, Macia L. The role of short-chain fatty acids in health and disease. Adv Immunol 2014;121:91–119.
[55] Matthews GM, Howarth GS, Butler RN. Short-chain fatty acid modulation of apoptosis in the Kato III human gastric carcinoma cell line. Cancer Biol Ther 2007;6(7):1051–7.
[56] Wang W, Fang D, Zhang H, Xue J, Wangchuk D, Du J, Jiang L. Sodium butyrate selectively kills cancer cells and inhibits migration in colorectal cancer by targeting thioredoxin-1. Onco Targets Ther 2020;13:4691–704.
[57] Sun Y, Sun Y, Yue S, Wang Y, Lu F. Histone deacetylase inhibitors in cancer therapy. Curr Top Med Chem 2018;18(28):2420–8.
[58] Tan Y, Jin Y, Wang Q, Huang J, Wu X, Ren Z. Perilipin 5 protects against cellular oxidative stress by enhancing mitochondrial function in HepG2 cells. Cells 2019;8(10).
[59] Oelkrug R, Goetze N, Meyer CW, Jastroch M. Antioxidant properties of UCP1 are evolutionarily conserved in mammals and buffer mitochondrial reactive oxygen species. Free Radic Biol Med 2014;77:210–6.
[60] Dillon LM, Bean JR, Yang W, Shee K, Symonds LK, Balko JM, McDonald WH, Liu S, Gonzalez-Angulo AM, Mills GB, Arteaga CL, Miller TW. P-REX1 creates a positive feedback loop to activate growth factor receptor, PI3K/AKT and MEK/ERK signaling in breast cancer. Oncogene 2015;34(30):3968–76.
[61] Chandra J, Amin HM, Howard A, Miller CP, Lin Q, Ban K. Fyn Upregulation Is a Novel ROS-Dependent Mechanism Controlling CML Growth, Progression and Imatinib Resistance. Am Soc Hematol 2006.
[62] Fu X-H, Chen C-Z, Wang Y, Peng Y-X, Wang W-H, Yuan B, Gao Y, Jiang H, Zhang J-B. COL1A1 affects apoptosis by regulating oxidative stress and autophagy in bovine cumulus cells. Theriogenology 2019;139:81–9.
[63] Myatt SS, Brosens JJ, Lam EW. Sense and sensitivity: FOXO and ROS in cancer development and treatment. Antioxid Redox Signal 2011;14(4):675–87.
[64] He Q, Gu L, Lin Q, Ma Y, Liu C, Pei X, Li PA, Yang Y. The Immp2l mutation causes ovarian aging through ROS-Wnt/β-catenin-estrogen pathway: preventive effect of melatonin. Endocrinology 2020;161(9):bqaa119.
[65] Hoste C, Dumont JE, Miot F, De Deken X. The type of DUOX-dependent ROS production is dictated by defined sequences in DUOXA. Exp Cell Res 2012;318(18):2353–64.
[66] Singh CK, Chhabra G, Ndiaye MA, Garcia-Peterson LM, Mack NJ, Ahmad N. The Role of Sirtuins in Antioxidant and Redox Signaling. Antioxid Redox Signal 2018;28(8):643–61.
[67] Grabowska W, Sikora E, Bielak-Zmijewska A. Sirtuins, a promising target in slowing down the ageing process. Biogerontology 2017;18(4):447–76.
[68] Anderson KA, Huynh FK, Fisher-Wellman K, Stuart JD, Peterson BS, Douros JD, Wagner GR, Thompson JW, Madsen AS, Green MF, Sivley RM, Ilkayeva OR, Stevens RD, Backos DS, Capra JA, Olsen CA, Campbell JE, Muoio DM, Grimsrud PA, Hirschey MD. SIRT4 is a lysine deacylase that controls leucine metabolism and insulin secretion. Cell Metab 2017;25(4):838–55. e15.
[69] Luo YX, Tang X, An XZ, Xie XM, Chen XF, Zhao X, Hao DL, Chen HZ, Liu DP. SIRT4 accelerates Ang II-induced pathological cardiac hypertrophy by inhibiting manganese superoxide dismutase activity. Eur Heart J 2017;38(18):1389–98.
[70] Bringman-Rodenbarger LR, Guo AH, Lyssiotis CA, Lombard DB. Emerging Roles for SIRT5 in Metabolism and Cancer. Antioxid Redox Signal 2018;28(8):677–90.
[71] Lu W, Zuo Y, Feng Y, Zhang M. SIRT5 facilitates cancer cell growth and drug resistance in non-small cell lung cancer. Tumour Biol 2014;35(11):10699–705.
[72] Ogura M, Nakamura Y, Tanaka D, Zhuang X, Fujita Y, Obara A, Hamasaki A, Hosokawa M, Inagaki N. Overexpression of SIRT5 confirms its involvement in deacetylation and activation of carbamoyl phosphate synthetase 1. Biochem Biophys Res Commun 2010;393(1):73–8.
[73] Bobermin LD, Wartchow KM, Flores MP, Leite MC, Quincozes-Santos A, Gonçalves CA. Ammonia-induced oxidative damage in neurons is prevented by resveratrol and lipoic acid with participation of heme oxygenase 1. Neurotoxicology 2015;49:28–35.
[74] Trachootham D, Alexandre J, Huang P. Targeting cancer cells by ROS-mediated mechanisms: a radical therapeutic approach? Nat Rev Drug Disco 2009;8(7):579–91.
[75] Traverso N, Ricciarelli R, Nitti M, Marengo B, Furfaro AL, Pronzato MA, Marinari UM, Domenicotti C. Role of glutathione in cancer progression and chemoresistance. Oxid Med Cell Longev 2013;2013:972913.
[76] Meister A. Glutathione deficiency produced by inhibition of its synthesis, and its reversal; applications in research and therapy. Pharm Ther 1991;51(2):155–94.
[77] Smith-Pearson PS, Kooshki M, Spitz DR, Poole LB, Zhao W, Robbins ME. Decreasing peroxiredoxin II expression decreases glutathione, alters cell cycle distribution, and sensitizes glioma cells to ionizing radiation and H(2)O(2). Free Radic Biol Med 2008;45(8):1178–89.
[78] Nkabyo YS, Ziegler TR, Gu LH, Watson WH, Jones DP. Glutathione and thioredoxin redox during differentiation in human colon epithelial (Caco-2) cells. Am J Physiol Gastrointest Liver Physiol 2002;283(6):G1352–9.
[79] Li N, Lewis P, Samuelson D, Liboni K, Neu J. Glutamine regulates Caco-2 cell tight junction proteins. Am J Physiol Gastrointest Liver Physiol 2004;287(3):G726–33.
[80] Louis M, Rosato RR, Brault L, Osbild S, Battaglia E, Yang XH, Grant S, Bagrel D. The histone deacetylase inhibitor sodium butyrate induces breast cancer cell apoptosis through diverse cytotoxic actions including glutathione depletion and oxidative stress. Int J Oncol 2004;25(6):1701–11.

[81] Kautenburger T, Beyer-Sehlmeyer G, Festag G, Haag N, Kühler S, Küchler A, Weise A, Marian B, Peters WH, Liehr T, Claussen U, Pool-Zobel BL. The gut fermentation product butyrate, a chemopreventive agent, suppresses glutathione S-transferase theta (hGSTT1) and cell growth more in human colon adenoma (LT97) than tumor (HT29) cells. J Cancer Res Clin Oncol 2005;131(10):692–700.
[82] Benard O, Balasubramanian KA. Modulation of glutathione level during butyrate-induced differentiation in human colon derived HT-29 cells. Mol Cell Biochem 1997;170(1–2):109–14.
[83] Konno M, Asai A, Kawamoto K, Nishida N, Satoh T, Doki Y, Mori M, Ishii H. The one-carbon metabolism pathway highlights therapeutic targets for gastrointestinal cancer (Review). Int J Oncol 2017;50(4):1057–63.
[84] Noguchi K, Konno M, Koseki J, Nishida N, Kawamoto K, Yamada D, Asaoka T, Noda T, Wada H, Gotoh K, Sakai D, Kudo T, Satoh T, Eguchi H, Doki Y, Mori M, Ishii H. The mitochondrial one-carbon metabolic pathway is associated with patient survival in pancreatic cancer. Oncol Lett 2018;16(2):1827–34.
[85] Martínez-Reyes I, Chandel NS. Mitochondrial one-carbon metabolism maintains redox balance during hypoxia. Cancer Disco 2014;4(12):1371–3.
[86] Kory N, Wyant GA, Prakash G, Uit de Bos J, Bottanelli F, Pacold ME, Chan SH, Lewis CA, Wang T, Keys HR, Guo YE, Sabatini DM. SFXN1 is a mitochondrial serine transporter required for one-carbon metabolism. Science 362. 2018.
[87] Pfendner W, Pizer LI. The metabolism of serine and glycine in mutant lines of Chinese hamster ovary cells. Arch Biochem Biophys 1980;200(2):503–12.
[88] McBurney MW, Whitmore GF. Isolation and biochemical characterization of folate deficient mutants of Chinese hamster cells. Cell 1974;2(3):173–82.
[89] Patel H, Pietro ED, MacKenzie RE. Mammalian fibroblasts lacking mitochondrial NAD+-dependent methylenetetrahydrofolate dehydrogenase-cyclohydrolase are glycine auxotrophs. J Biol Chem 2003;278(21):19436–41.
[90] Christie GR, Ford D, Howard A, Clark MA, Hirst BH. Glycine supply to human enterocytes mediated by high-affinity basolateral GLYT1. Gastroenterology 2001;120(2):439–48.
[91] Razak MA, Begum PS, Viswanath B, Rajagopal S. Multifarious beneficial effect of nonessential amino acid, glycine: a review. Oxid Med Cell Longev 2017;2017:1716701.
[92] Dang CV. MYC, metabolism, cell growth, and tumorigenesis. Cold Spring Harb Perspect Med 2013;3(8).
[93] Wise DR, DeBerardinis RJ, Mancuso A, Sayed N, Zhang XY, Pfeiffer HK, Nissim I, Daikhin E, Yudkoff M, McMahon SB, Thompson CB. Myc regulates a transcriptional program that stimulates mitochondrial glutaminolysis and leads to glutamine addiction. Proc Natl Acad Sci USA 2008;105(48):18782–7.
[94] Gao P, Tchernyshyov I, Chang TC, Lee YS, Kita K, Ochi T, Zeller KI, De Marzo AM, Van Eyk JE, Mendell JT, Dang CV. c-Myc suppression of miR-23a/b enhances mitochondrial glutaminase expression and glutamine metabolism. Nature 2009;458(7239):762–5.
[95] Osthus RC, Shim H, Kim S, Li Q, Reddy R, Mukherjee M, Xu Y, Wonsey D, Lee LA, Dang CV. Deregulation of glucose transporter 1 and glycolytic gene expression by c-Myc. J Biol Chem 2000;275(29):21797–800.
[96] David CJ, Chen M, Assanah M, Canoll P, Manley JL. HnRNP proteins controlled by c-Myc deregulate pyruvate kinase mRNA splicing in cancer. Nature 2010;463(7279):364–8.
[97] Gan L, Xiu R, Ren P, Yue M, Su H, Guo G, Xiao D, Yu J, Jiang H, Liu H, Hu G, Qing G. Metabolic targeting of oncogene MYC by selective activation of the proton-coupled monocarboxylate family of transporters. Oncogene 2016;35(23):3037–8.
[98] Bekebrede AF, Deuren TV, Gerrits WJJ, Keijer J, Boer VCJ. Butyrate alters pyruvate flux and induces lipid accumulation in cultured colonocytes. Int J Mol Sci 2021;22(20).
[99] Tappenden KA, Thomson AB, Wild GE, McBurney MI. Short-chain fatty acid-supplemented total parenteral nutrition enhances functional adaptation to intestinal resection in rats. Gastroenterology 1997;112(3):792–802.
[100] Drozdowski LA, Dixon WT, McBurney MI, Thomson AB. Short-chain fatty acids and total parenteral nutrition affect intestinal gene expression. JPEN J Parent Enter Nutr 2002;26(3):145–50.
[101] Wang G, Yu Y, Wang YZ, Wang JJ, Guan R, Sun Y, Shi F, Gao J, Fu XL. Role of SCFAs in gut microbiome and glycolysis for colorectal cancer therapy. J Cell Physiol 2019;234(10):17023–49.
[102] Smolle M, Prior AE, Brown AE, Cooper A, Byron O, Lindsay JG. A new level of architectural complexity in the human pyruvate dehydrogenase complex. J Biol Chem 2006;281(28):19772–80.
[103] Tan Z, Xie N, Banerjee S, Cui H, Fu M, Thannickal VJ, Liu G. The monocarboxylate transporter 4 is required for glycolytic reprogramming and inflammatory response in macrophages. J Biol Chem 2015;290(1):46–55.
[104] Weng Y, Fan X, Bai Y, Wang S, Huang H, Yang H, Zhu J, Zhang F. SLC2A5 promotes lung adenocarcinoma cell growth and metastasis by enhancing fructose utilization. Cell Death Disco 2018;4:38.
[105] Chen WL, Wang YY, Zhao A, Xia L, Xie G, Su M, Zhao L, Liu J, Qu C, Wei R, Rajani C, Ni Y, Cheng Z, Chen Z, Chen SJ, Jia W. Enhanced fructose utilization mediated by SLC2A5 is a unique metabolic feature of acute myeloid leukemia with therapeutic potential. Cancer Cell 2016;30(5):779–91.
[106] Ciuchi E, Odetti P, Prando R. Relationship between glutathione and sorbitol concentrations in erythrocytes from diabetic patients. Metabolism 1996;45(5):611–3.
[107] Hedtke V, Bakovic M. Choline transport for phospholipid synthesis: An emerging role of choline transporter-like protein 1. Exp Biol Med (Maywood) 2019;244(8):655–62.
[108] Green CR, Wallace M, Divakaruni AS, Phillips SA, Murphy AN, Ciaraldi TP, Metallo CM. Branched-chain amino acid catabolism fuels adipocyte differentiation and lipogenesis. Nat Chem Biol 2016;12(1):15–21.
[109] Moffatt BA, Ashihara H. Purine and pyrimidine nucleotide synthesis and metabolism. Arab Book 2002;1:e0018.
[110] Chaumeil MM, Najac C, Ronen SM. Studies of metabolism using 13C MRS of hyperpolarized probes. Methods Enzymol 2015;561:1–71.